JGR Biogeosciences

RESEARCH ARTICLE
10.1029/2025JG009332

Consistent Spectral Reflectance Signatures of Photosystem II Thermal Tolerance (T_{crit}) in Contrasting Foundation Tree Species

Benjamin C. Wiebe[1], Madeline E. Moran[2,3], Megan M. Seeley[4], Rebecca Senft[5], Alexandra Schuessler[2], Eleanor R. Thomson[6], Luiza M. T. Aparecido[5], Hillary F. Cooper[7], Catherine A. Gehring[7], Kevin R. Hultine[2], Dan F. Koepke[2], Roberta E. Martin[4], Bradley C. Posch[2,8], Andrew D. Richardson[1,9], Thomas G. Whitham[7], Gerard J. Allan[7], Gregory P. Asner[4], and Christopher E. Doughty[1]

[1]School of Informatics, Computing, and Cyber Systems, Northern Arizona University, Flagstaff, AZ, USA, [2]Department of Research, Conservation and Collections, Desert Botanical Garden, Phoenix, AZ, USA, [3]School of Life Sciences, Arizona State University, Tempe, AZ, USA, [4]Center for Global Discovery and Conservation Science, Arizona State University, Hilo, HI, USA, [5]School of Biological Sciences, University of Utah, Salt Lake City, UT, USA, [6]School of Geography & the Environment, University of Oxford, Oxford, UK, [7]Department of Biological Sciences and Center for Adaptable Western Landscapes, Northern Arizona University, Flagstaff, AZ, USA, [8]Department of Environmental Science, Policy and Management, University of California Berkeley, Berkeley, CA, USA, [9]Center for Ecosystem Science and Society, Northern Arizona University, Flagstaff, AZ, USA

Abstract Photosystem II (PSII) is among the most thermally sensitive components of photosynthesis, and emerging evidence suggests that plants in diverse biomes face an increasing risk of PSII damage under future climate change. However, uncertainties in the distribution and drivers of PSII thermal tolerance (T_{crit}) limit our ability to predict thermal risk in plant communities across spatial scales. Here, we evaluate whether intraspecific variation in T_{crit} corresponds to leaf reflectance spectra (400–2,500 nm) to identify mechanisms associated with T_{crit} in field conditions and assess the potential of its estimation using remote sensing platforms. We measured T_{crit} using temperature response curves of minimal fluorescence (F_o) along with corresponding leaf reflectance spectra in two foundation tree species: *Populus fremontii* (US Southwest) and *Metrosideros polymorpha* (Hawai'i). *P. fremontii* was sampled under both moderate (<40°C) and extreme (>45°C) heat. Consistent spectral signatures of T_{crit} emerged across species and sampling conditions, with the strongest signatures in *P. fremontii* under extreme heat. In *P. fremontii,* spectra captured up to roughly half of T_{crit} variation and allowed T_{crit} estimation (R^2 = 0.24–0.30; RMSE < 1.0°C) and classification of high-versus low-T_{crit} (71%–77% accuracy). Across both species, T_{crit} tended to increase with spectral indices reflecting higher chlorophyll content and lower carotenoids, nonphotochemical quenching, and leaf water content. These findings suggest that variation in PSII thermal tolerance is linked to fundamental biochemical properties of leaves, which are reflected in their optical traits. As climate extremes intensify, spectral screening and scaling of T_{crit} via remote sensing may support improved conservation, management, and risk assessment in vulnerable ecosystems.

Plain Language Summary Plant communities are critical for the Earth system, but many face increasing pressures in a changing climate. One key risk is that plants may reach temperatures that damage their photosynthetic machinery. However, thermal tolerance varies widely between species and individuals, making it difficult to assess plant vulnerability at a scale. Here we test whether thermal tolerance can be predicted from how leaves reflect light at different wavelengths—a method known as leaf spectroscopy that captures key leaf traits and can be scaled using remote sensing platforms. We tested this approach in two distinct tree species: *Populus fremontii* from the U.S. Southwest and Metrosideros polymorpha from Hawai'i. Despite their differences, both showed similar spectral patterns linked to the temperature at which photosynthesis begins to break down. These signatures suggested that plants with higher thermal tolerance tend to have more chlorophyll and less leaf water and protective pigments than plants with lower tolerance. In P. fremontii, leaf spectra explained up to approximately half of the variation in thermal tolerance and predicted high versus low tolerance with 70%–80% accuracy. These results help understand the mechanisms associated with thermal tolerance in the field, and may support landscape-scale assessments of plant vulnerability to heat using remote sensing.

Key Points:

- Leaf reflectance spectra (400–2,500 nm) show consistent signatures of PSII thermal tolerance (T_{crit}) in contrasting species and conditions
- In *Populus fremontii*, spectra predicted T_{crit} (R^2 = 0.24–0.3; RMSE < 1°C) and classified high versus low T_{crit} with 71%–77% accuracy
- Spectral indices suggest T_{crit} is positively correlated with chlorophyll content; negatively correlated with water and carotenoid content

Supporting Information:

Supporting Information may be found in the online version of this article.

Correspondence to:

B. C. Wiebe and C. E. Doughty,
bcw269@nau.edu;
chris.doughty@nau.edu

Citation:

Wiebe, B. C., Moran, M. E., Seeley, M. M., Senft, R., Schuessler, A., Thomson, E. R., et al. (2026). Consistent spectral reflectance signatures of photosystem II thermal tolerance (T_{crit}) in contrasting foundation tree species. *Journal of Geophysical Research: Biogeosciences*, *131*, e2025JG009332. https://doi.org/10.1029/2025JG009332

Received 4 AUG 2025
Accepted 4 FEB 2026

Author Contributions:

Conceptualization: Benjamin C. Wiebe, Kevin R. Hultine, Christopher E. Doughty
Data curation: Benjamin C. Wiebe, Christopher E. Doughty
Formal analysis: Benjamin C. Wiebe, Christopher E. Doughty
Funding acquisition: Catherine A. Gehring, Kevin R. Hultine, Thomas G. Whitham, Gerard J. Allan, Gregory P. Asner, Christopher E. Doughty
Investigation: Benjamin C. Wiebe, Madeline E. Moran, Rebecca Senft, Alexandra Schuessler, Eleanor R. Thomson, Luiza M. T. Aparecido, Hillary F. Cooper, Kevin R. Hultine, Dan

F. Koepke, Bradley C. Posch, Christopher E. Doughty
Methodology: Benjamin C. Wiebe, Madeline E. Moran, Megan M. Seeley, Rebecca Senft, Alexandra Schuessler, Andrew D. Richardson, Christopher E. Doughty
Project administration: Christopher E. Doughty
Resources: Kevin R. Hultine, Roberta E. Martin, Andrew D. Richardson, Christopher E. Doughty
Software: Benjamin C. Wiebe
Supervision: Christopher E. Doughty
Visualization: Benjamin C. Wiebe
Writing – original draft: Benjamin C. Wiebe
Writing – review & editing: Benjamin C. Wiebe, Madeline E. Moran, Megan M. Seeley, Rebecca Senft, Alexandra Schuessler, Eleanor R. Thomson, Luiza M. T. Aparecido, Hillary F. Cooper, Catherine A. Gehring, Kevin R. Hultine, Dan F. Koepke, Roberta E. Martin, Bradley C. Posch, Andrew D. Richardson, Thomas G. Whitham, Gerard J. Allan, Gregory P. Asner, Christopher E. Doughty

1. Introduction

Rising global temperatures and intensifying heat waves associated with anthropogenic climate change pose a growing threat to plant photosynthesis in terrestrial ecosystems (IPCC, 2021; Russo et al., 2014). Leaf temperature, which often exerts a stronger influence than air temperature on physiological processes such as photosynthesis and respiration, can significantly exceed air temperature during periods of high solar irradiance (Doughty & Goulden, 2009; Still et al., 2022). While moderately high leaf temperatures can cause temporary reductions in plant productivity (Doughty & Goulden, 2009; Koch et al., 1994; Sharkey, 2005), recent research in tropical (Doughty et al., 2023; Tiwari et al., 2021), temperate (Still et al., 2023), arid (Moran et al., 2023), and even boreal (Rao et al., 2023) regions has found that many plant canopies are likely nearing and occasionally surpassing temperatures damaging to photosynthetic biochemistry and leaf tissue. However, these upper temperature limits vary significantly across regions, species, and individuals, and temporally through diurnal and seasonal cycles (Posch et al., 2022), complicating predictions of how ecosystems will respond to rising temperatures (Doughty et al., 2023).

Photosystem II (PSII) is among the most thermally sensitive components of photosynthesis. Extreme heat destabilizes thylakoid membranes, damages core protein complexes, and impairs charge separation at the reaction center (Mathur et al., 2014; Schreiber & Berry, 1977). This damage increasingly redirects chlorophyll excitation energy toward fluorescence, allowing fluorescence to be used to quantify thermal tolerance (Knight & Ackerly, 2002; Schreiber & Berry, 1977; Yamane et al., 1997). A leaf's critical temperature (T_{crit}) can be estimated in the lab by heating dark-adapted leaf discs in water and tracking minimal fluorescence (F_o). T_{crit} is identified as the temperature at which F_o begins to rise sharply (e.g., Figure 1e), and corresponds to disruption to the light-harvesting antenna and the PSII core complex (Knight & Ackerly, 2002; Schreiber & Berry, 1977). Although surpassing T_{crit} does not always cause leaf death (Winter et al., 2025), it likely requires repair to restore photosynthetic function and therefore marks a key metabolic threshold (Hüve et al., 2006; Tóth et al., 2011). Like other biological thresholds, T_{crit} depends on both intensity (i.e., temperature) and exposure duration; therefore, it should not necessarily be interpreted as a strict upper temperature limit for leaf survival (Cook et al., 2024). However, when measured consistently, it remains a robust metric for comparing thermal tolerance across plants (Knight & Ackerly, 2002; O'Sullivan et al., 2017).

Plants exhibit significant variation in T_{crit} and therefore may show variable responses to increasing heat exposure with climate change. T_{crit} generally increases with temperature across elevational and latitudinal gradients, but variation in T_{crit} among co-occurring species often exceeds these broad trends, creating potential "winners" and "losers" within plant communities (Bison & Michaletz, 2024; Feeley et al., 2020; O'sullivan et al., 2017). In addition to interspecific differences, T_{crit} can vary considerably among populations and individuals of the same species (Coast et al., 2022; Middleby et al., 2025). This variation, compounded by limited T_{crit} sampling across many species and regions, limits the ability to predict plant community responses to future high temperature extremes (Doughty et al., 2023).

The mechanisms associated with variation in T_{crit} within and among species also remain only partly understood. While T_{crit} has been linked to traits associated with the leaf economic spectrum, such as leaf mass per area (LMA), these relationships are inconsistent across studies and environments (Bison & Michaletz, 2024; O'sullivan et al., 2017; Sastry & Barua, 2017; Slot et al., 2020). Other mechanisms shown to influence T_{crit} include leaf fatty acid composition, and protective compounds such as zeaxanthin, heat shock proteins, and osmolytes (Havaux, 1998; Heckathorn et al., 1998; Zhu et al., 2018). However, the extent to which these mechanisms explain observed variation in T_{crit}, both within and among species, is largely unknown (Feeley et al., 2020; Zhu et al., 2018).

The goal of this study was to explore the physiological basis of intraspecific variation in T_{crit} and assess the potential for predicting T_{crit} using remote sensing, which could provide a cost-effective landscape-scale approach for assessing thermal risk. This knowledge is especially important for foundation tree species that structure ecosystems and support a wide range of sensitive or endangered taxa (Ellison et al., 2005). By leveraging how leaf structure and chemistry influence light absorption and scattering properties, leaf spectroscopy can enable rapid assessment of key traits (Asner & Martin, 2008; Gamon et al., 1992; Richardson et al., 2002) and provide the foundation for scaling these predictions with remote sensing (Asner et al., 2015; Gamon et al., 2019). However, it remains unclear whether spectral signatures of thermal tolerance exist, and if so, whether they are consistent across species, environments, and heat exposure.

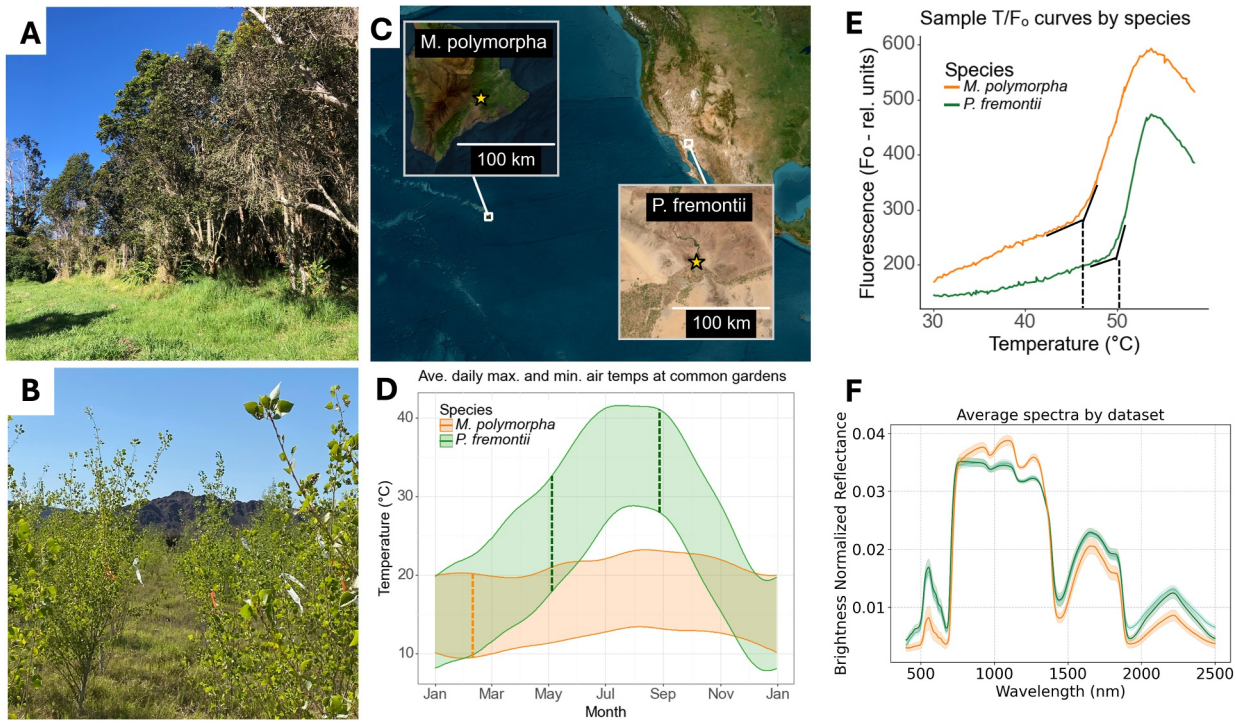

Figure 1. Overview of sampling locations and measurements used in this experiment. Site (a) *Metrosideros polymorpha* common garden near Volcano, Hawaii (photo: B. Wiebe); (b) *Populus fremontii* common garden near Yuma, Arizona (photo: L. Aparecido); (c) Map of common garden locations (yellow stars); (d) Seasonal variations in average daily minimum and maximum air temperatures (1991–2020) (*Source: NOAA*). Vertical dashed lines represent the sampling times for each species. (e) Sample T/F_o curves used to obtain T_{crit} (dashed lines) from each species. (f) Average and standard deviation brightness normalized leaf reflectance spectra by species.

Several mechanisms could link leaf reflectance spectra to T_{crit}. First, spectroscopy might detect leaf traits that directly influence T_{crit}, such as beta-carotene concentrations, which increase thylakoid membrane fluidity and decrease T_{crit}, and which directly influence leaf reflectance spectra (Gitelson et al., 2002; Havaux, 1998). Second, spectroscopy might capture traits which correlate with other traits that directly influence T_{crit}. For example, spectroscopy can predict nitrogen concentrations, which may be correlated with heat shock proteins which confer higher thermal tolerance (Kokaly, 2001; Wang et al., 2014). Similarly, spectroscopy can predict leaf water content, which is correlated with osmolyte concentrations, which itself can increase thermal tolerance (Das et al., 2018; Hüve et al., 2006). Third, to the degree that T_{crit} varies by provenance/population in these two species, spectroscopy might be able to adequately predict T_{crit} simply by predicting provenance (Corbin et al., 2024; Seeley et al., 2025). Finally, spectroscopy might measure photosynthetic or oxidative stress responses that arise when individuals in a shared hot environment experience differing degrees of thermal stress due to variations in T_{crit} (Tafesse et al., 2022). Multiple stress responses are detectable by spectroscopy, including decreased chlorophyll concentration (Carter & Knapp, 2001) or de-epoxidation of xanthophyll-cycle pigments (Gamon et al., 1992). Although zeaxanthin accumulation can stabilize thylakoid membranes under heat stress (Havaux, 1998), its primary role is photoprotection via nonphotochemical quenching (Demmig-Adams et al., 2020), and it often accompanies heat stress (Behnke et al., 2007). In combination, these four examples/pathways suggest multiple opportunities to use leaf reflectance to detect variations in T_{crit} in field conditions.

We examined the relationship between T_{crit} and leaf reflectance spectra (400–2,500 nm) in two phylogenetically distinct model tree species, *Populus fremontii* and *Metrosideros polymorpha*, grown in common gardens in their contrasting native habitats (US Southwest and Hawaii, respectively). We selected these species for their contrasting phylogenies (orders: Malpighiales vs. Myrtales), evolutionary histories (Choi et al., 2021; Liu et al., 2022), and environmental selection pressures (Moran et al., 2023; Seeley & Asner, 2023), primarily to examine the generalizability of spectral trends in environmentally and phylogenetically distinct species. While *M. polymorpha* is a tropical evergreen species that grows on volcanic soils in the relatively stable climate of the

Hawaiian Islands (Cordell et al., 1998; Stacy & Johnson, 2021), *P. fremontii* is a temperate deciduous species that occupies continental alluvial soils in the American Southwest, where large seasonal temperature swings can push ambient air temperatures beyond 45°C (Hartwell et al., 2010; Moran et al., 2023). Both are foundation tree species that span wide temperature gradients and exhibit substantial genotypic and phenotypic variation—variation that is partially retained in the common garden settings used here (Corbin et al., 2024; Martin et al., 2007). Conducting this study in common gardens minimized confounding environmental effects on spectral-T_{crit} relationships and allowed the assessment of whether population- or individual-level variation shaped observed relationships. Since *P. fremontii* frequently experiences extreme summer temperatures that exceed 45°C, including at the site of its common garden (Yuma, Arizona; Moran et al., 2023), we evaluated spectral-T_{crit} relationships in that species in both spring and summer to assess whether high temperature exposure impacts these relationships.

Specifically, we address the following questions:

- Q1. Do spectral signatures of T_{crit} exist, and if so, are they consistent in different species and growing temperatures?
- Q2. To what extent does population- or individual-level variation shape relationships between reflectance spectra and T_{crit}?
- Q3. Is T_{crit} correlated with known spectral indices of pigment concentrations, nonphotochemical quenching, or leaf water content, or with inferred leaf traits from a leaf radiative transfer model?
- Q4. Can leaf spectra accurately predict intraspecific variation in T_{crit}?

2. Methods

We used two established common gardens—one for *P. fremontii* near Yuma, Arizona (Cooper et al., 2018) and one for *M. polymorpha* near Volcano, Hawaii (Cordell et al., 1998)—to assess the relationships between T_{crit} and leaf reflectance (400–2,500 nm). An overview of the sites and methods used can be found in Figure 1. We sampled *M. polymorpha* in a single field campaign (February 2023), but sampled *P. fremontii* twice (May and August 2021) to compare spectral-T_{crit} relationships in the same trees under moderate (<40°C) and extreme (>45°C) heat (Moran et al., 2023). For each data set, we analyzed spectral trends and indices, compared how much variation in thermal tolerance each spectral region captured, and tested the ability of reflectance spectra to predict and classify T_{crit}.

2.1. Study Sites

Populus fremontii common garden—A *P. fremontii* common garden was established near Yuma, Arizona (32.850 N, 114.493 W, 49 m a.s.l) in 2014 using cuttings from 16 populations of *P. fremontii* from across Arizona that represent the full elevation and temperature range of both the Sonoran Desert ecotype and the southern range of the Utah High Plateau ecotype (Bothwell et al., 2023; Ikeda et al., 2017). This garden has been described in greater detail in Cooper et al. (2018), Hultine et al. (2020), and Moran et al. (2023). We selected eight populations from the Sonoran Desert ecotype spanning 70–1,234 m source elevation and maximum temperature of the warmest month from 34.2°C to 42.6°C (Fick & Hijmans, 2017), corresponding to the populations used in Moran et al. (2023). We sampled in both spring (May 3–6) and summer (August 20–22, 2021). The average daily minimum/maximum air temperatures at the garden in the 1-month period preceding each collection were 16.3/32.4°C in spring (reaching 39°C on 30 April 2021) and 29.2/40.2°C in summer (reaching 47°C on 3 August 2021).

Metrosideros polymorpha common garden—A common garden was established at the Hawai'i Volcano Experimental Station in Volcano, HI (19.476 N, 155.260 W, 1,190 m a.s.l.) in 1994 from seeds collected from 10 populations of *M. polymorpha* across an elevation gradient (107–2,469 m a.s.l.; mean annual temperatures between 10 and 23°C) along the eastern slopes of Mauna Loa volcano (Cordell et al., 1998). Detailed information regarding the establishment of this garden can be found in Cordell et al. (1998) and Martin et al. (2007). We selected seven populations spanning the entire elevation range of the species (Table S1 in Supporting Information S1). We sampled between February 9 and 14, 2023. Average daily minimum/maximum air temperatures at the garden in the month preceding collection were 18.1/27.5°C (reaching 30.6°C on 20 January 2023).

Table 1
Number of Trees and Leaves Used for Leaf Spectral Measurements and T_{crit} Measurement in Each Data Set, Along With Number of Total Spectral Scans and Temperature/Fluorescence Curves Used

Data set	Number of trees (unit of analysis)	Leaves used for spectra	Total spectra	Leaves for T_{crit}	Total T-F_o curves
P. fremontii –Yuma (May)	69	339	1,018	298	894
P. fremontii—Yuma (Aug)	59	294	882	187	559
M. polymorpha—common garden	31	275	825	111	332

Note. Since T_{crit} and leaf spectra were associated at the level of the tree, this was the unit of analysis, and all data from individual leaves and scans were averaged by tree before performing analysis.

2.2. Leaf Collections

We collected a total of 1,118 *P. fremontii* and 386 M. *polymorpha* leaves for spectral and T_{crit} measurements (Table 1). In the *P. fremontii* common garden, we sampled nine sunlit canopy leaves from each tree: four to five for spectral measurements and three to four for T_{crit}. We sampled a total of 69 trees in May 2021 and 59 in August 2021. Sampling in May was at least ∼60 days after spring leaf-out dates reported for this garden (Cooper et al., 2018). Since *P. fremontii* continues to flush new leaves throughout the growing season (Moran et al., 2023), leaves were likely of similar ages in the two sampling periods. As trees were under three m tall, we sampled leaves by hand using hand pruners in the mid to late afternoon and stored them in a dark cooler (∼10°C). We stored leaves for spectra in coin envelopes in the dark for >1 hr before measuring spectra later that afternoon or evening. Leaves for T_{crit} measurements were stored in Ziplock bags with a few drops of water to keep them moist and shipped T_{crit} leaves (same day) to the Desert Botanical Garden (DBG, Phoenix, AZ) and processed them within 72 hr (Moran et al., 2023).

For *M. polymorpha*, we collected 12 sunlit canopy leaves mid-morning from each of 31 trees using a 10-m pole pruner. We used three to four leaves per tree for T_{crit} measurements and nine for spectral measurements. We immediately placed the leaves in Ziplock bags and stored them in a dark cooler (∼20°C). We measured leaf spectra of dark-acclimated leaves on the same day as collection. We overnight shipped T_{crit} leaves to DBG in padded boxes to prevent damage or extreme temperature exposure, with branchlets or petioles placed in capped floral water vials/tubes (Royal Imports; Brooklyn, NY, USA) filled with water to keep them hydrated. All shipments were received the morning after collection and processed within an additional 48 hr. Because T_{crit} was to be measured at DBG after shipping, the maximum quantum yield (F_v/F_m) of *M. polymorpha* leaves was measured before transport using a Fluorpen 100 (Photon Systems Instruments, Drásov, Czechia) and after the shipments at DBG with a FC800-C FluorCam (Photon Systems Instruments, Drásov, Czechia) to assess the stress induced by shipping. F_v/F_m remained high (∼0.8) after shipping, indicating minimal stress during transport.

2.3. Leaf Reflectance Spectra Measurements

We measured leaf reflectance spectra using an ASD FieldSpec 3 spectrometer (Analytical Spectral Devices Inc., Boulder, CO, USA) and a broadleaf clip. Leaves were stored in coin envelopes in the dark for >1 hr prior to experiencing the bright light of the spectrometer during measurement. We scanned the adaxial surface, avoiding the midrib. Spectra were recorded between 350 and 2,500 nm at 1 nm intervals and trimmed to 400–2,500 nm to reduce edge noise. We measured three spectra for each *P. fremontii* leaf and one spectrum for each *M. polymorpha* leaf since *M. polymorpha* leaves are smaller and often only big enough for one independent spectrum using the broadleaf clip. Each spectrum was averaged from 10+ scans. We collected white references between trees and convert radiance to reflectance. We corrected for sensor temperature sensitivity at 1,000 and 1,830 nm using parabolic corrections (Hueni & Bialek, 2017) and brightness-normalized each spectrum by dividing each wavelength by the spectrum norm (Feilhauer et al., 2010; Wang et al., 2020). We used normalized spectra in all analyses (main text figures), but repeated key steps using raw spectra to confirm that normalization did not greatly alter the results (SI). Raw spectra aggregated by data set are shown in Figure S1 of Supporting Information S1.

2.4. T_{crit} Measurements

We measured T_{crit} using the temperature-dependent rise in minimal fluorescence (F_o) of dark-adapted leaves, as described in Schreiber and Berry (1977), Berry and Bjorkman (1980), Knight and Ackerly (2002), and more

recently in Posch et al. (2024) and Moran et al. (2023). After at least 30 min of dark adaptation, three 5.5 mm diameter leaf discs from each leaf were placed within a 48-well Peltier heating block, along with 0.9 ml of water per well. Samples were heated from 30°C to 60°C at 0.5°C min^{-1} by a TR2000 thermoregulator (Photon Systems Instruments, Drásov, Czechia), with F_o of leaf discs measured every 30 s by a FC800-C FluorCam (Photon Systems Instruments, Drásov, Czechia). T_{crit} was defined as the temperature inflection point at which F_o began to rapidly increase (Schreiber & Berry, 1977), calculated using the "segmented" R package (version 1.6-4). F_o curves were inspected visually and curves with uncharacteristic shapes or excessive noise were removed from the analysis.

Recent research has reported that strong light (1,000 $\mu mol \cdot m^{-2} \cdot s^{-1}$) reduces leaf thermal tolerance (Nie et al., 2025); therefore, this approach using dark acclimated leaves may be overestimating thermal tolerance relative to in situ values. However, given that all leaves underwent the same protocol, we do not expect this or other potential biases from our lab-based T_{crit} measurements to impact the reported relationships between T_{crit} and spectra.

2.5. Data Analysis

Since leaf spectra and T_{crit} were related at the tree level, we averaged all spectral scans and T_{crit} measurements from each tree before conducting the analyses. We performed all analyses separately for each data set: *M. polymorpha*, *P. fremontii* (May), and *P. fremontii* (August). All analyses were performed in Python (3.9.12), using numpy (1.25.0), pandas (1.5.3), scipy (1.10.1), statsmodels (0.14.0), matplotlib (3.7.2), seaborn (0.12.2), plotnine (0.12.3), scikit-learn (1.0.2), and prosail (2.0.5). Before relating T_{crit} to reflectance spectra, we first calculated the average and standard deviation of T_{crit} in each data set. We then used simple linear regression to test whether T_{crit} was associated with population source elevation, and one-way ANOVA to assess whether T_{crit} differed significantly among populations. We report η^2 as a measure of population effect size, representing the proportion of variance in T_{crit} explained by population.

While we used tree-averaged spectra and T_{crit} for all analyses, we also quantified leaf-level variability in both spectra and T_{crit}, relative to tree-level variability. We did this by calculating the standard deviation (SD) of both T_{crit} and reflectance at each wavelength among leaves within individual trees (leaf-level SD) and the standard deviation of tree means for both T_{crit} and reflectance (tree-level SD) and comparing both to the total standard deviation across all leaves for both traits. This was done separately for each data set. This helped contextualize our tree-level analysis and evaluate the potential importance of leaf-level variability on spectral-T_{crit} relationships.

2.5.1. Q1: Spectral Signatures of T_{crit}

To assess wavelength-dependent spectral reflectance correlations with T_{crit}, we calculated the correlations (r) between reflectance at each wavelength and T_{crit}, and plotted these correlations, differentiating significant versus non-significant correlations. However, simple correlations treat each wavelength in isolation and ignore covariation among wavelengths. To account for these interactions and identify spectral regions that contribute most to explaining T_{crit}, we used Variable Importance in Projection (VIP) scores derived from partial least squares regression (PLSR) (using *scikit-learn*). PLSR extracts components or latent variables that maximize covariance with the response variable and fits a linear model to these components, while VIP scores summarize the relative contribution of each wavelength to the model, weighted by the amount of variance explained by each component (Chong & Jun 2005). We used the first two PLSR components (Doughty et al., 2011) trained on the whole spectrum (400–2,500 nm) to calculate VIP scores. A VIP score of 1 is commonly used as a threshold for indicating significance for PLSR models, with VIP scores above 1 indicating above average contribution to the model (Chavana-Bryant et al., 2017).

While VIP scores account for collinearity and highlight which individual wavelengths contribute most to explaining T_{crit}, they do not reveal how reflectance at given wavelengths relates to reflectance at other specific wavelengths. To visualize pairwise relationships between specific wavelengths, we calculated normalized difference indices (NDIs) across broad spectral ranges and plotted their correlations with T_{crit} as correlograms (Balzarolo et al., 2018; Peñuelas et al., 1995).

The general normalized difference index format is as follows:

Table 2
Narrowband Spectral Indices Used in the Analysis, Which Relate to Pigment Concentrations and Ratios, and Leaf Water Content

Spectral index	Formula	Physiological significance	Citation
Green normalized difference vegetation index (GNDVI)	$GNDVI = \frac{R_{750} - R_{550}}{R_{750} + R_{550}}$	Sensitive to chlorophyll concentration	Gitelson et al. (2002)
Chlorophyll normalized difference index (ChlNDI)	$ChlNDI = \frac{R_{750} - R_{705}}{R_{750} + R_{705}}$	Highly correlated with chlorophyll concentration	Richardson et al. (2002)
Photochemical reflectance index (PRI)	$PRI = \frac{R_{531} - R_{570}}{R_{531} + R_{570}}$	Can indicate "facultative" changes in the epoxidation status of xanthophyll cycle pigments or "constitutive" changes in chlorophyll/carotenoid ratio	Gamon et al. (1992), Gamon et al. (1997); Gamon and Berry (2012)
Structure-independent pigment index (SIPI)	$SIPI = \frac{R_{800} - R_{445}}{R_{800} + R_{680}}$	Correlated with carotenoid to chlorophyll *a* ratio	Penuelas (1995)
Red Edge Position (REP) (λ_{RE})	$REP = Wavelength\ of\ maximum\ first\ derivative\ between\ 680$-740 nm	Sensitive to chlorophyll concentration, leaf structure, and water status	HORLER et al. (1983)
Normalized difference water index (NDWI)	$NDWI = \frac{R_{860} - R_{1240}}{R_{860} + R_{1240}}$	Correlated with plant water content	Stimson et al. (2005)

Note. R_x is spectral reflectance at x nanometers. Significance of each index and key citations are also given.

$$\mathrm{NDI} = \frac{R_a - R_b}{R_a + R_b} \quad (1)$$

where R_a and R_b are normalized reflectance values at wavelengths a and b, respectively. This allows the quick visual analysis of many wavelength combinations. For example, just considering reflectance at wavelengths 400–1,000 nm (x 1 nm), there are 180,000 normalized index combinations of wavelengths a and b, and considering 400–2,500 nm, there are 2.2 million combinations. We plotted correlations between T_{crit} and these indices, with the first wavelength of the index represented by the y-axis and the second wavelength of the index represented by the x-axis. This allows comparisons of spectral signatures in different data sets (i.e., *M. polymorpha*; *P. fremontii* in May and August), and helps to assess whether spectral indices of leaf chemistry (Table 2) capture the main correlations between leaf spectra and T_{crit}.

2.5.2. Q2: Contribution of Population-Versus Individual-Level Variation

To evaluate whether spectral-T_{crit} relationships were shaped by population-level differences or individual variation, we fit linear mixed effects (using *statsmodels*) models using three components from a full-spectrum PLSR model as fixed effects, with population included as a random effect. This approach accounts for the possibility that populations differ both in T_{crit} and in spectral traits, which could yield spectral-T_{crit} relationships unrelated to thermal tolerance itself. From each model, we calculated random effect variance, residual variance, and the intra-class correlation coefficients (ICCs), which quantify the proportion of total variance in each fixed effect attributable to population-level differences (Nakagawa et al., 2017). To summarize these effects, we averaged ICCs across components within each species and sampling period, providing an estimate of the degree to which observed spectral-T_{crit} relationships reflect population-level versus individual-level variation.

2.5.3. Q3: T_{crit}, Spectral Indices, and Inferred Leaf Traits

To explore possible mechanistic connections between spectra and T_{crit}, we first assessed correlations between established spectral indices related to photosynthetic pigments, non-photochemical quenching (NPQ), and leaf

water content (Table 2). We fit simple linear regression models relating each index to T_{crit} and extracted the correlation coefficient (r), slope, and *p*-value to assess the strength, direction, and significance of each relationship.

Next, we inferred biochemical and structural leaf traits using leaf radiative transfer inversion using the PROSPECT model (Jacquemoud et al., 2009) using the *prosail* python package. PROSPECT simulates directional hemispherical reflectance and transmittance of a leaf as a function of its internal structure parameter (N), pigment pools (chlorophyll and carotenoids), brown pigments, liquid water thickness, and dry matter content. PROSPECT inversion modeling has been shown to accurately estimate leaf traits (Jiang et al., 2018). One advantage of PROSPECT over simple vegetation indices (e.g., normalized difference vegetation index and photochemical reflectance index), is that it estimates leaf internal structure, such as "N," the structure parameter used in PROSPECT to represent the number of air/cell wall interfaces within the mesophyll and dry matter content. We passed raw reflectance spectra (400–2,500 nm) into PROSPECT-D and estimated the parameters listed above by minimizing the squared difference between measured and modeled reflectance using a least squares optimizer (*scipy.optimize.least_squares*). From estimated chlorophyll and carotenoid concentrations we calculated Carotenoid:Chlorophyll ratio. As with spectral indices, we calculated and plotted correlations between these inferred traits and T_{crit} (*r*).

2.5.4. Q4: Predicting T_{crit} With Leaf Spectra

To evaluate the predictive potential of leaf reflectance spectra for PSII thermal tolerance (T_{crit}), we first found the within-sample fit of partial least squares regression (PLSR) models (*scikit-learn*) using tree-averaged reflectance data from four spectral regions: visible (VIS: 400–700 nm), near-infrared (NIR: 700–1,300 nm), shortwave-infrared (SWIR: 1,300–2,500 nm), and the full spectrum (400–2,500 nm). The number of PLSR components was determined by minimizing the Prediction Residual Error Sum of Squares (PRESS) statistic, calculated using a leave-one-out cross-validation procedure (Asner et al., 2015; Chen et al., 2004), and was capped at 5 components. Root mean square error (RMSE) and the coefficient of determination (R^2; Chicco et al., 2021) of the resulting PLSR models were calculated for each data set and spectral region.

To assess the out-of-sample predictive accuracy of PLSR, we implemented nested 5-fold cross-validation. In each iteration, the outer loop held out a test set of trees, while the inner loop selected the optimal number of components (up to 10) based on the validation RMSE. Performance was evaluated using RMSEP and R^2, averaged across folds by data set and spectral region.

Lastly, we tested whether leaf spectra could classify trees as having above- or below-median T_{crit} using partial least squares discriminant analysis (PLS-DA). This approach, similar to heat tolerance phenotyping efforts in crops using other measurements (Sharma et al., 2015), serves as a proof of concept for spectral phenotyping, with possible applications in identifying heat-tolerant populations or genotypes for restoration. Within each training fold, trees were classified based on whether their T_{crit} exceeded the training-set median. Prediction accuracy of held-out trees within the test data set was calculated and averaged across folds. This approach used the same nested 5-fold cross-validation framework described above and included the same spectral regions for comparison.

3. Results

P. fremontii T_{crit} was 48.8 ± 1.2°C in May 2021 and 50.1 ± 0.8°C in August 2021. *M. polymorpha* exhibited lower thermal tolerance than *P. fremontii* in either month, with a mean T_{crit} of 45.7 ± 1.6°C. We found directionally similar spectral signatures of T_{crit} across species and growth temperatures, with the strongest signals observed in *P. fremontii* under extreme summer heat (August). These relationships were primarily driven by individual-level variation rather than population-level structuring. Spectral signatures were generally strongest and most consistent in the visible region, and were generally well captured by established pigment-related indices, suggesting similar associations between T_{crit} and photochemistry across data sets. PLSR models explained 38% and 47% of intraspecific variation in T_{crit} in *P. fremontii* (within-sample fit) in August and May, respectively, allowing out-of-sample predictions (R^2: 0.24–0.30) and classification of high-versus low T_{crit} (71%–77% accuracy) within that species.

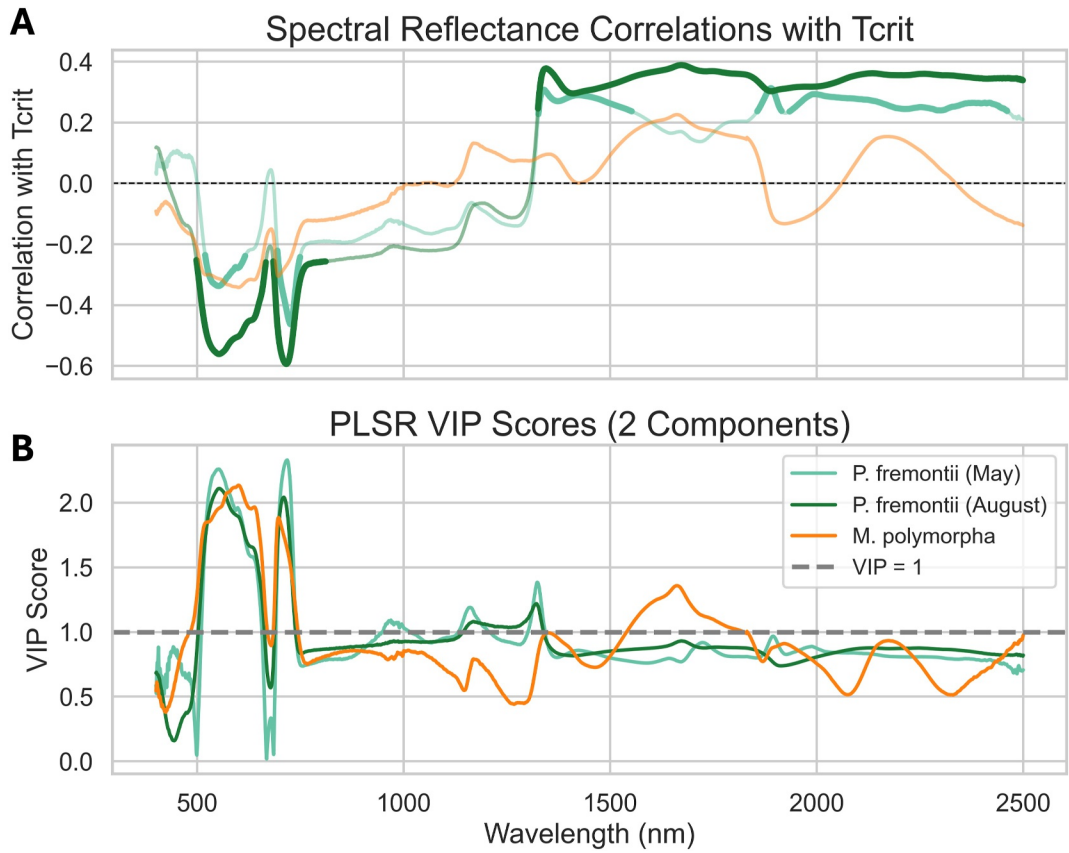

Figure 2. (a) Spectral correlations with T_{crit} by data set, with significant correlations bolded. Consistent correlations are found across data sets in the visible and red-edge regions (~500–750 nm), with strongest correlations in *P. fremontii* measured in August (b) Variable importance in projection (VIP) scores for a partial least squares regression (PLSR) T_{crit} model with 2 components. Wavelengths with VIP scores above one are considered significant for the T_{crit} PLSR model. Across species and sampling conditions, PLSR identified green (~550–600 nm) and red-edge (~700–750 nm) wavelengths as most important for capturing T_{crit} variation.

3.1. Q1: Spectral Signatures of T_{crit}

We found consistent spectral signatures of T_{crit} across species and growth temperatures (Figure 2). In all data sets, visible to near-infrared (V-NIR) regions contributed most to the PLSR models, as indicated by high (>1) VIP scores, with particularly high importance in the green (~550–600 nm) and red edge (~690–720 nm) wavelengths (Figure 2b; Figure S2b in Supporting Information S1). These same regions showed significant negative correlations between T_{crit} and reflectance in both *P. fremontii* data sets, particularly in August with negative correlations reaching −0.59 when canopy temperatures exceeded 45°C and approached average August T_{crit} values of 50.1 ± 0.8°C (Figure 2a; Figure S2a in Supporting Information S1). While visible to near-infrared regions were found to be most important in PLSR models according to VIP scores and showed the most consistent patterns across data sets, reflectance in large portions of the shortwave infrared (SWIR) region was significantly correlated with T_{crit} in *P. fremontii* ($r > 0.2$; $p < 0.05$), especially under extreme heat in August (Figure 2a). Although reflectance was not correlated with T_{crit} at any single wavelength in *M. polymorpha* ($p < 0.05$), the overall correlation pattern in the visible to red-edge regions resembled that of *P. fremontii*.

Normalized difference index (NDI) correlograms further supported these findings by capturing pairwise reflectance comparisons. In all data sets, T_{crit} was significantly correlated with indices contrasting green versus longer-wavelength green (e.g., reversed-wavelength PRI), with the clearest expression in *M. polymorpha* (Figure 3 and Figure S3 in Supporting Information S1; NDI correlograms with only significant correlations presented in Figure S4 of Supporting Information S1). In both *P. fremontii* data sets, T_{crit} was also positively correlated with indices comparing red edge versus green/yellow, NIR versus green (e.g., GNDVI) and NIR versus

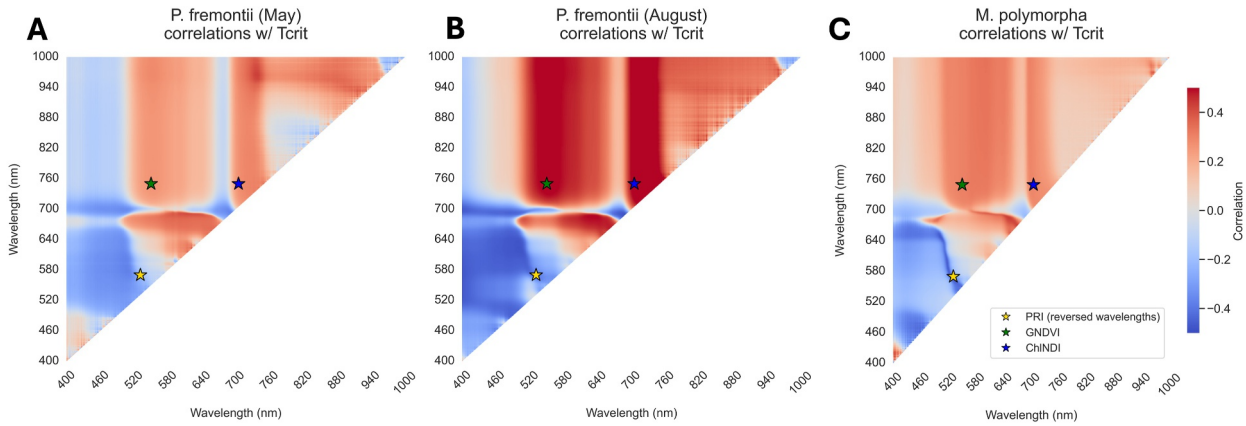

Figure 3. Correlograms of visible to near-infrared spectral indices related to T_{crit} for *P. fremontii* sampled in May (a) and August (b) and for *M. polymorpha* (c). Each pixel represents the normalized difference index ($[R_1 - R_2]/[R_1 + R_2]$) between the wavelength on the *y*-axis (R_1) and the wavelength on the *x*-axis (R_2) (180,000 indices visualized between 400 and 1,000 nm). Stars represent several spectral indices used in this analysis that only use two wavelengths, with some wavelength orders reversed, changing the sign of the relationship. Similarities in spectral patterns emerge across species and sampling conditions, and several key spectral indices related to pigments and photochemistry (i.e., GNDVI, ChlNDI and PRI) generally capture some of the main spectral features across data sets.

red edge (e.g., ChlNDI), with the strongest relationships again found in the August *P. fremontii* data set. These latter patterns were visibly evident but non-significant in *M. polymorpha* (Figure 3; Figures S3 and S4 in Supporting Information S1).

3.2. Q2: Contribution of Population-Versus Individual-Level Variation

Spectral-T_{crit} relationships were primarily driven by individual-level variation, though the extent of population-level structuring varied across data sets. Population source elevation explained little of the variation in T_{crit}: 6% in *P. fremontii* in May ($R^2 = 0.06$), 2% in August ($R^2 = 0.02$), and none in *M. polymorpha* ($R^2 = 0.00$). Population identity, however, accounted for more substantial variation, particularly in *P. fremontii* during May, where population explained 48% of T_{crit} variance ($\eta^2 = 0.48$; $p < 0.001$). This was lower in *P. fremontii* in August ($\eta^2 = 0.08$) and in *M. polymorpha* ($\eta^2 = 0.069$). A visualization of T_{crit} by population and data set is provided in Figure S5 in Supporting Information S1.

These results are consistent with mixed effects models treating population as a random effect. In both *P. fremontii* (August) and *M. polymorpha*, intra-class correlation coefficients (ICCs < 0.01) indicated that nearly all of the T_{crit} variation captured by spectra was attributable to tree-level differences rather than population-level structuring. In contrast, population structure played a substantial role in *P. fremontii* measured in May (ICC = 0.44; Table 3; Table S2 in Supporting Information S1), suggesting that in *P. fremontii* under moderate thermal conditions, spectral-T_{crit} relationships were more strongly mediated by population-level differences.

While we could not directly relate spectra with T_{crit} at the leaf level, we could compare leaf- and tree-level variability in both spectra and T_{crit} to contextualize these results. In *P. fremontii*, leaf-level (within-canopy) spectral variation was greater in August than in May, but in both months, leaf-level spectral variation was similar in magnitude to tree-level (among-canopy) standard deviation across the spectrum (Figure S6a in Supporting Information S1). T_{crit} showed a similar partitioning, with comparable contributions from leaf- and tree-level

Table 3
Variance Components and ICCs From Mixed Effects Models Assessing the Contribution of Population-Level Differences to Spectral-T_{crit} Relationships

Data set	Random effect (population) variance	Residual variance	Intra-class correlation coefficient (ICC)
P. fremontii (May)	0.544	0.704	0.436
P. fremontii (August)	0.000391	0.450	0.000868
M. polymorpha	0.000143	2.649	0.0000539

Note. Population effects were substantial in *P. fremontii* (May) but negligible in *P. fremontii* (August) and *M. polymorpha*.

variability, though overall T_{crit} variation was greater in May than in August (Figure S6b in Supporting Information S1). In *M. polymorpha*, most spectral variation was attributable to tree-level differences, with consistently greater tree-than leaf-level variability across wavelengths. In contrast, T_{crit} variability in *M. polymorpha* was driven more by leaf-level than tree-level variability (Figures S6a and S6b in Supporting Information S1).

3.3. Q3: T_{crit}, Spectral Indices, and Inferred Leaf Traits

Across data sets, T_{crit} was generally correlated with spectral indices related to chlorophyll content, carotenoid: chlorophyll ratio, non-photochemical quenching (NPQ), and leaf water content, though correlations were not always significant (Figure 4a; Figure S7 and Table S3a in Supporting Information S1). Correlations were strongest and most consistent in *P. fremontii* (August), where T_{crit} was positively associated with predicted chlorophyll content (ChlNDI, GNDVI) and red edge position (REP) and negatively related to predictions of carotenoid:chlorophyll ratio (SIPI), NPQ (PRI), and leaf water content (NDWI). Individual indices explained up to ~30% of the variation in T_{crit} in this data set. In *P. fremontii* (May), significant correlations were observed with indices related to chlorophyll content (ChlNDI, GNDVI) and red edge position (REP), whereas in *M. polymorpha*, only PRI was significantly associated with T_{crit}. Slopes, correlation coefficients (r), coefficient of determination (R^2), and *p*-values for each regression model are presented in Table S3a of Supporting Information S1.

PROSPECT inversion modeling yielded similar trait-T_{crit} patterns to those observed using spectral indices (Figure 4b). In *P. fremontii*, higher T_{crit} was associated with higher inferred chlorophyll $a + b$ content, and lower carotenoid:chlorophyll ratio, consistent with the index results above. In *P. fremontii* (August), T_{crit} was also negatively correlated with inferred leaf water thickness. These relationships were directionally similar across species and months, although not always statistically significant. Inferred carotenoid content itself showed non-significant positive correlations with T_{crit} in all data sets. Because PROSPECT also estimates structural traits not recoverable from narrowband indices, we also examined relationships with the PROSPECT leaf structure parameter (N) and inferred dry matter content. T_{crit} was significantly positively correlated with N in *P. fremontii* (May). Correlations with dry matter content diverged across data sets, with a positive relationship in *P. fremontii* (May) but a negative relationship in *M. polymorpha*. Full statistics for individual trait models (slopes, r, R^2, *p*-values) are shown in Table S3b of Supporting Information S1, while summary statistics of PROSPECT inferred leaf traits by data set are presented in Table S4 of Supporting Information S1.

3.4. Q4: Predicting T_{crit} With Leaf Spectra

Leaf reflectance spectra explained 17%–47% of intraspecific variation in T_{crit} in *P. fremontii*, depending on sampling period and spectral range, and this explanatory power translated into reliable out-of-sample predictions and classifications in this species (Table 4; Figures 5 and 6; Figures S8 and S9 in Supporting Information S1). Within-sample PLSR models showed the strongest performance in *P. fremontii* (May), where near infrared models (700–1300 nm) explained up to 47% of the variation (within-sample $R^2 = 0.47$; RMSE = 0.63; $p < 0.0001$), likely due to the strong population-level structuring in this data set (see Q2 above) and the ability of spectra to differentiate populations of *P. fremontii* both in the wild and in common gardens with high (>70%) accuracy (Corbin et al., 2024; Seeley et al., 2025). In *P. fremontii* (August), within-sample R^2 ranged from 32% to 38% ($p < 0.001$), with the visible region performing best. For *M. polymorpha*, PLSR explained <12% of T_{crit} variation, and models were not significant.

Out-of-sample PLSR prediction, evaluated via nested cross-validation and held-out samples, was lower overall but retained predictive power in *P. fremontii* (Figure 5; Figure S8 in Supporting Information S1). Under extreme summer conditions (August), models explained up to 31% of variation in the test data set. In May, only NIR-based PLSR models predicted T_{crit} in the test data set ($R^2 = 0.24$). In contrast, no spectral region yielded out-of-sample predictions ($R^2 > 0$) in *M. polymorpha*. The results above are from when we relate T_{crit} and spectra at the leaf level; results relating T_{crit} and spectra at the leaf level are presented in Figure S10 of Supporting Information S1. Results from PLSR models using only wavelengths were found to be most important in Figure 2 (VIP score > 1) are presented in Figure S11 in Supporting Information S1.

Classification models predicting whether T_{crit} exceeded the training-set median were similarly more successful in *P. fremontii* than in *M. polymorpha*. Using PLS-DA, visible wavelengths predicted above-versus below-average T_{crit} with 71% accuracy in August, while NIR-based models reached 77% accuracy in May. No spectral region

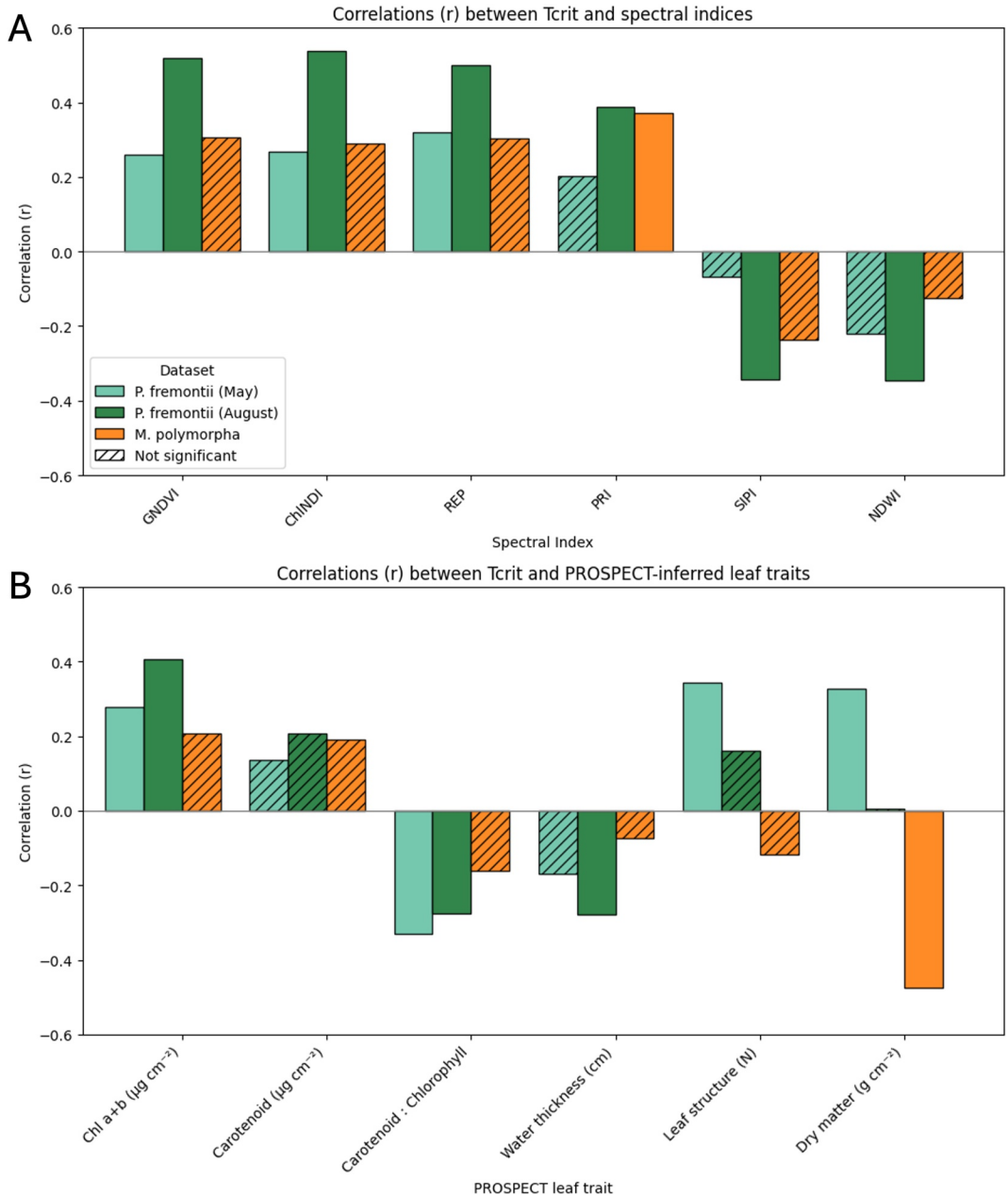

Figure 4. (a) Correlations (r) between T_{crit} and indices related to chlorophyll content (GNDVI and ChlNDI), chlorophyll content and leaf structure (REP), facultative and/or constitutive components of the xanthophyll cycle (PRI), carotenoid: chlorophyll *a* ratios (SIPI), and leaf water content (NDWI). Directionally similar correlations were observed across data sets, but with varying magnitudes and significance levels. Strongest correlations were found in *P. fremontii* measured under extreme heat (>45°C) in August, but were still present in *P. fremontii* in cooler conditions (<40°C) and in *M. polymorpha*. (b) Correlations (r) between T_{crit} and leaf traits inferred from PROSPECT inversion modeling. Results are consistent with correlations with indices from (a), with T_{crit} positively correlated with inferred chlorophyll *a* and *b* and negatively correlated with carotenoid: chlorophyll ratio and water thickness. Species diverged in their correlations with inferred leaf dry matter content, with positive correlations with T_{crit} in *P. fremontii* (May) and negative correlations in *M. polymorpha.*

produced significant classification accuracy (i.e., reliably above 50%) in *M. polymorpha* (Table 4; Figure 6; Figure S9 in Supporting Information S1).

We tested model generalizability across species and sampling period in the SI (Text S1 in Supporting Information S1: "Testing spectral model generalizability between species and contexts"). Models trained in one

Table 4
Model Results by Data Set and Spectral Range (VIS, Visible; NIR, Near Infrared; SWIR, Shortwave Infrared; ALL, Full Spectrum)

Data set	Range	Within-sample PLSR R^2	Within-sample PLSR RMSE	Within-sample PLSR num. comps.	Mean out-of-sample PLSR R^2	Mean out-of-sample PLSR RMSE	Mean pls-DA classification accuracy
P. fremontii (May)	VIS	0.168	1.084	3	−0.175	1.230	0.622
	NIR	0.469	0.866	5	0.238	0.982	0.768
	SWIR	0.339	0.966	5	−0.143	1.191	0.625
	ALL	0.253	1.027	3	−0.116	1.183	0.668
P. fremontii (August)	VIS	0.379	0.632	3	0.269	0.666	0.712
	NIR	0.369	0.637	3	0.305	0.649	0.644
	SWIR	0.319	0.661	4	0.111	0.733	0.629
	ALL	0.347	0.648	3	0.195	0.701	0.644
M. polymorpha	VIS	0.091	1.591	1	−0.430	1.676	0.576
	NIR	0.031	1.642	1	−0.804	1.843	0.538
	SWIR	0.066	1.612	2	−0.472	1.789	0.538
	ALL	0.110	1.574	2	−0.631	1.783	0.548

Note. Within-sample models used the full data set, with the number of latent variables or components determined using leave-one-out cross validation. Out-of-sample PLSR and PLS-DA model results represent the mean across five-fold cross-validation, with the number of components used in each fold determined via nested cross validation within each fold.

species did not transfer to the other, but some transferability between May and August was achieved in *P. fremontii*. Notably, 2-band spectral indices (ChlNDI, PRI) achieved modest high versus low T_{crit} classification across species and seasons (55%–63% accuracy), suggesting that low-complexity spectral features may generalize across contexts better than more complex models (e.g., PLSR), although training models across multiple species and context would also likely help create a more generalizable model.

4. Discussion

We found consistent spectral signatures of T_{crit} in contrasting foundation tree species, indicative of coherent associations with pigment concentrations and photochemistry. While signals were strongest in *P. fremontii* exposed to extreme temperatures (>45°C), allowing the most reliable out-of-sample T_{crit} estimation, they were still present, and directionally similar, in *P. fremontii* at lower temperatures (<40°C) and in *M. polymorpha*. Below, we explore the likely physiological basis of these spectral-T_{crit} relationships, their functional significance for heat tolerance, their possible reflection of shared evolutionary constraints on photosynthesis, and implications for remote sensing and high-throughput phenotyping of thermal tolerance.

4.1. Ecophysiology and Photochemistry in Moderate and Extreme Temperatures

The main goal of this study was to explore the physiological basis of intraspecific variation in leaf thermal tolerance using relationships with leaf spectra. While spectra do not capture all meaningful leaf trait variation, we found consistent relationships between T_{crit} and spectral signatures associated with pigment content and photochemical processes across species and temperature regimes. Because absorption by photosynthetic pigments dominates spectral reflectance signatures in visible and red-edge wavelengths (Jacquemoud et al., 2009), the high VIP scores in these regions (Figure 2b) suggest that photochemistry is the main link between T_{crit} and leaf spectral signatures. Moreover, because spectra captured up to roughly half of T_{crit} variation, depending on the data set, our results indicate that pigments and photochemistry represent major correlates of leaf thermal tolerance within species.

Under both moderate (<40°C) and extreme (>45°C) conditions, T_{crit} was generally positively correlated with indications of chlorophyll content (e.g., GNDVI, ChlNDI; predictions from inverted PROSPECT modeling), and with PRI. Since higher PRI values can reflect either lower carotenoid content or reduced NPQ, this relationship suggests less reliance on photoprotective pigment accumulation and energy dissipation in more heat-tolerant trees (Demmig-Adams et al., 2020; Gamon & Berry, 2012). Although leaves were measured after a dark acclimation

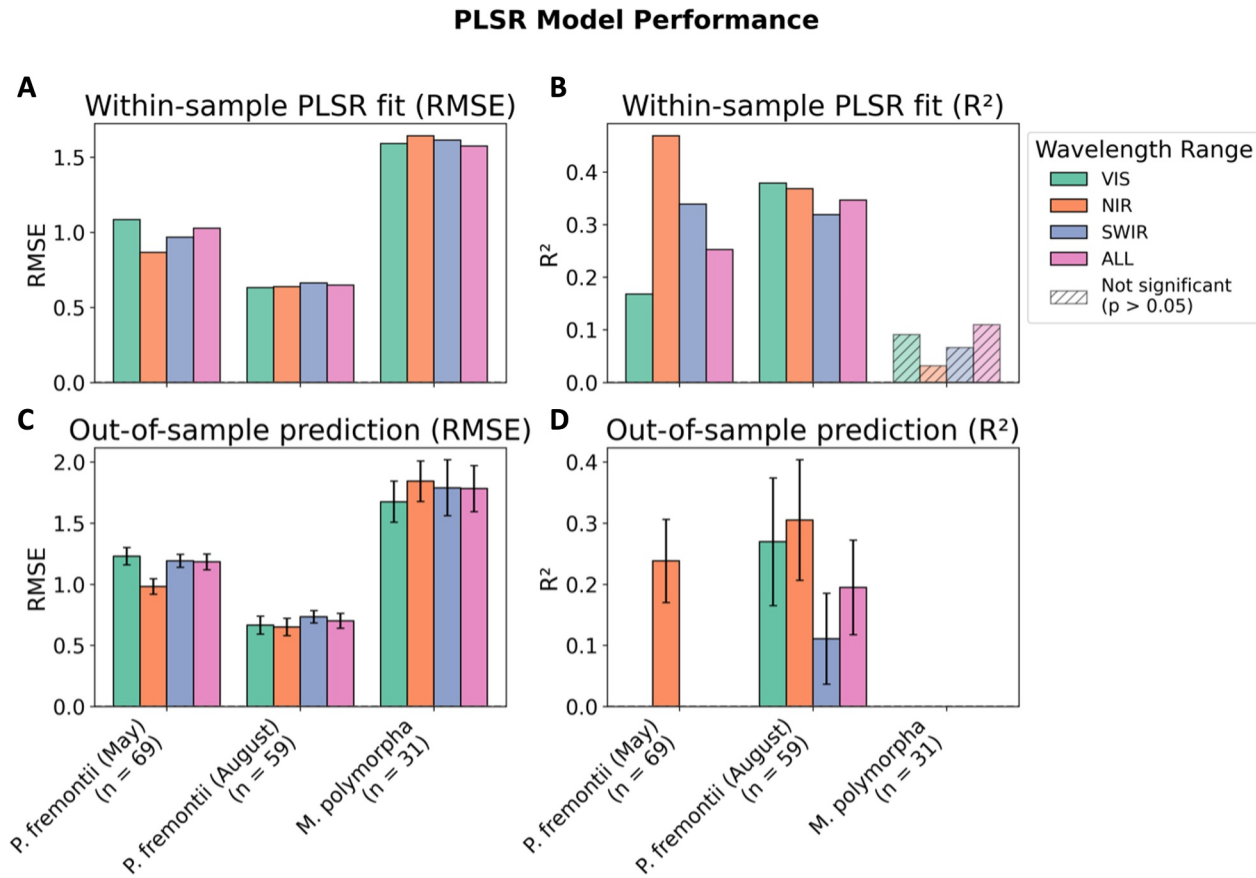

Figure 5. Partial least squares regression (PLSR) model performance by spectral range and data set. Root mean squared error (RMSE) (a) and coefficient of determination (R^2) (b) for within-sample PLSR models. PLSR captured 17%–47% of T_{crit} variation in *P. fremontii*, depending on the spectral region used. Out-of-sample prediction RMSE (c) and R^2 (d) for PLSR models (≤5 components), aggregated across 5-folds of cross validation, with R^2 values below zero removed for clarity. Out-of-sample prediction was achieved in *P. fremontii* but not *M. polymorpha*. Legend code: VIS, visible (400–700 nm); NIR, near infrared (700–1,300 nm); SWIR, shortwave infrared (1,300–2,500 nm).

period, either facultative or constitutive components of PRI still could have contributed to this correlation, as residual zeaxanthin pools have been shown to persist in the dark for up to several hours following long-duration high-light stress (Kress & Jahns, 2017). While statistical significance of relationships varied across data sets, the directionality of relationships between spectral indices and T_{crit} was the same in all cases, suggesting consistent physiological and spectral relationships with T_{crit} across species and growth temperatures.

In the extreme temperatures *P. fremontii* experienced in August, spectral signatures associated with T_{crit} most likely reflect variations in physiological heat stress. T_{crit} was inversely correlated with spectral indications of stress (e.g., chlorophyll degradation, elevated carotenoid levels, increased NPQ), consistent with extensive evidence that heat stress induces such responses (Behnke et al., 2007; Carter & Knapp, 2001; Demmig-Adams et al., 2020; Dhami & Cazzonelli, 2020; Wang et al., 2018). In addition to indicating heat stress, these responses can serve adaptive roles: chlorophyll breakdown mitigates oxidative damage from overexcited chlorophyll (Wang et al., 2018), while carotenoids and NPQ dissipate excess energy, protecting the PSII reaction center (Demmig-Adams, 1990).

These results suggest that T_{crit} is a relevant metric for plant performance at high temperatures, even if experienced temperatures do not exceed T_{crit} or lead to leaf necrosis. Leaf temperatures likely did not reach T_{crit} or higher in this experiment, as reported by Moran et al. (2023), and did not cause visible leaf necrosis; however, in *P. fremontii*, they did exceed temperatures known to induce temporary PSII disruptions (~35–40°C; Sharkey, 2005; Tiwari et al., 2021). These temporary disruptions can prompt protective mechanisms (Tiwari et al., 2021; Wang et al., 2018) similar to those likely evident in the spectra in this study. Since plant

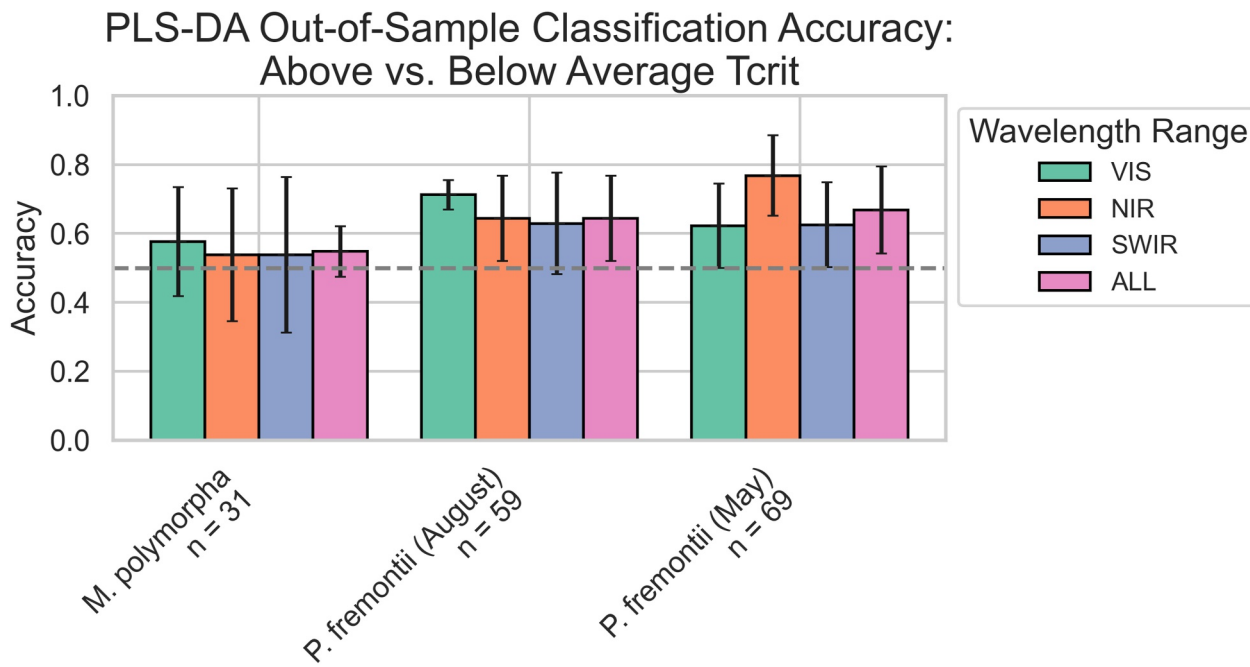

Figure 6. Out-of-sample classification accuracy for above- versus below-median T_{crit}, using partial least squares discriminant analysis (PLS-DA). Visible wavelengths (400–700 nm) achieved 71% accuracy in *P. fremontii* measured in August, while near infrared wavelengths (700–1,300 nm) achieved 77% accuracy in *P. fremontii* in May. Classification accuracies above 50% were not achieved in *M. polymorpha*. Legend code: VIS, visible (400–700 nm); NIR, near infrared (700–1,300 nm); SWIR, shortwave infrared (1,300–2,500 nm).

susceptibility to transient PSII disruptions at moderately high temperatures and more permanent PSII damage at extreme temperatures are influenced by shared physiological factors (e.g., thylakoid membrane fluidity and leakiness; Havaux, 1998; Sharkey, 2005), the spectral signatures of T_{crit} observed here likely reflect tolerance to both moderate and extreme heat stress.

Similar pigment-based stress responses have been previously identified in crop varieties differing in thermal tolerance. Heat-sensitive varieties often exhibit increased shifts in pigment composition under heat stress, whereas tolerant varieties tend to maintain chlorophyll. This pattern has been observed across crops ranging from hot peppers, tomatoes, wheat, and peas (Rajametov et al., 2021; Sharma et al., 2015; Tafesse et al., 2022; Zhou et al., 2017). However, to our knowledge, our study provides the first demonstration of similar relationships between spectral signatures, inferred pigment composition, and thermal tolerance across individuals of a wild tree species (*P. fremontii*) exposed to temperatures approaching their thermal limits (i.e., ~50°C).

While spectral patterns under extreme temperatures primarily reflect variable stress responses, the weaker yet directionally consistent relationships observed at moderate temperatures likely correspond to photochemical traits directly influencing thermal tolerance. Chlorophyll-rich pigment-protein complexes, such as LHCIIb, can enhance PSII thermal tolerance by stabilizing the thylakoid membrane and oxygen-evolving complexes (Havaux & Tardy, 1997; Shutilova et al., 1995). Given that LHCIIb binds a substantial portion (~40%) of total leaf chlorophyll (Havaux & Tardy, 1997), spectral indicators of chlorophyll may indirectly reflect structural contributions to thermal stability. Conversely, certain carotenoids, such as ß-carotene, can increase thylakoid membrane fluidity and reduce thermal tolerance (Havaux, 1998), potentially explaining negative correlations with indications of carotenoid content at moderate temperatures.

While we primarily focus on spectral signatures related to photochemistry, we also found significant relationships between T_{crit} and spectral indicators of leaf water content and structure. Correlations with predicted leaf water content were significant only in *P. fremontii* in August, but the other data sets showed directionally similar trends, consistent with recent work reporting negative associations between leaf thermal tolerance and leaf water content across species (Valliere et al., 2023). We also found contrasting correlations between T_{crit} and PROSPECT-inferred leaf mass per area (LMA; "dry matter content"), with positive correlations in *P. fremontii* (May) but

negative correlations in *M. polymorpha*. The positive relationship in *P. fremontii* is consistent with studies showing that higher LMA can be associated with higher T_{crit} across species (Sastry & Barua, 2017; Slot et al., 2020), and here we show that this pattern can also arise intraspecifically. In contrast, the negative correlation in *M. polymorpha* may reflect the inverse relationship between LMA and mass-based nitrogen concentrations described by Martin et al. (2007) in this same common garden, as nitrogen can enhance thermal tolerance (Wang et al., 2014). While future work would be needed to test this mechanism directly, these results suggest that LMA itself is unlikely to determine T_{crit}; instead, it likely covaries with other biochemical traits that more directly mediate thermal tolerance.

The spectral signatures and possible physiological explanations presented here reflect between-canopy and intraspecific relationships, but we also found leaf-level variability in both T_{crit} and spectra within individual canopies. Given that many of the underlying physiological and photochemical traits likely underpinning spectral-T_{crit} relationships operate at the leaf level (e.g., Wang et al., 2018), we would expect similar relationships to exist within canopies. However, confirming this would require future studies that relate spectra and T_{crit} at the level of individual leaves.

4.2. Ecology and Evolutionary History

Given the distinct evolutionary histories of *P. fremontii* and *M. polymorpha* (Choi et al., 2021; Liu et al., 2022) and the contrasting thermal environments they inhabit (Blasini et al., 2022; Martin & Asner, 2009; Moran et al., 2023), these species might be expected to have evolved divergent physiological strategies for dealing with heat stress, and therefore exhibit distinct spectral signatures associated with T_{crit}. However, while we did find varying degrees of investment into thermal tolerance (T_{crit}: 45.7 ± 1.7°C vs. 49.4 ± 1.1°C for *M. polymorpha* and *P. fremontii*, respectively) and varying strengths of spectral signals associated with T_{crit}, we found that these species exhibit directionally consistent spectral signatures of T_{crit}, especially in visible wavelengths linked to pigments and photochemistry. This similarity can be seen in the similar PLSR VIP scores and reflectance correlations (Figure 2), correlation patterns with normalized difference indices (Figure 3), and similar directionality for correlations with pigment indices (although with inconsistent statistical significance) (Figure 4).

This convergence may reflect evolutionary constraints on the photosynthetic apparatus and conservation of mechanisms influencing photosynthesis and thermal tolerance. Prior work has shown that key photosynthetic traits and their spectral signatures are often conserved across lineages (Meireles et al., 2020; Ollinger, 2011), suggesting that there are fundamental biophysical constraints on photosynthesis (Meireles et al., 2020). While T_{crit} varies considerably between species and individuals, we suggest that the underlying physiological mechanisms by which plants adjust thermal tolerance may be broadly similar across diverse lineages, allowing T_{crit}-spectral relationships to also remain relatively consistent.

While T_{crit} appears only weakly related to deep evolutionary history and phylogeny, it may still exhibit structure over shorter evolutionary timescales, such as among populations or provenances within species. In this study, we found that variation among populations differed according to species and ambient conditions. In *P. fremontii*, population-level differences in T_{crit} were substantial in May, with ICCs indicating that nearly half of the explainable variation was attributable to population identity. By August, however, this structure disappeared (ICC < 0.01), likely due to convergence under extreme heat stress (Moran et al., 2023; Posch et al., 2024). In contrast, *M. polymorpha* showed minimal population-level structuring under moderate temperatures (ICC < 0.01), consistent with higher potential for gene flow than *P. fremontii* (Choi et al., 2021; Cushman et al., 2014) and likely lower selection pressure for extreme heat tolerance (Stacy et al., 2014). These results align with findings from other common garden studies showing that provenance effects on T_{crit} are species-specific (Middleby et al., 2025). Notably, across both structured and unstructured contexts, we observed consistent spectral signatures of T_{crit}, suggesting that spectroscopy captures physiological mechanisms directly linked to thermal tolerance, rather than merely reflecting population-level correlations between spectra and T_{crit}.

4.3. Leveraging Spectral Signatures of T_{crit} for Remote Sensing and Phenotyping

Spectral signatures of T_{crit} were consistent across species and enabled modest predictive accuracy in *P. fremontii*, with the strongest predictions under extreme heat. Out-of-sample models explained 24%–31% of T_{crit} variation and classified trees with above- or below-median T_{crit} with 71%–77% accuracy. In contrast, despite having increased T_{crit} variability for spectroscopy to leverage (standard deviation: 1.6°C), *M. polymorpha* showed little

predictive signal. This is likely due to limited tree-level sample size ($n = 31$), or simply lower investment into thermal tolerance in *M. polymorpha*, meaning spectral signals are harder to detect. These results suggest that leaf reflectance spectroscopy might help scale predictions of thermal tolerance to canopy levels, particularly in hot environments. In turn, remote sensing and subsequent rapid phenotyping of heat-tolerant genotypes have the potential to enhance the success of restoration, agriculture, or other managed ecosystems exposed to hot conditions.

Current and upcoming imaging spectrometers offer increasing potential to estimate foliar traits at landscape scales. These include pigment concentrations, non-photochemical quenching (NPQ), and canopy water content—all traits found here to correlate with T_{crit} under high-temperature conditions (Asner & Martin, 2008; Cawse-Nicholson et al., 2021; Gamon et al., 2019; Green et al., 2020; Seeley & Asner, 2023). However, scaling T_{crit} predictions with imaging spectroscopy must contend with key challenges related to spatial resolution, environmental variability, and the context-dependence of stress-related spectral signals. For example, current hyperspectral satellite sensors lack the spatial resolution to resolve tree-to-tree variation in T_{crit}. Further, across broad climate gradients, co-occurring increases in thermal tolerance and stress signals (e.g., chlorophyll degradation, NPQ; Corbin et al., 2024) may confound the spectral-T_{crit} relationship found here. In our controlled settings, T_{crit} was inversely correlated with the indications of photosynthetic stress. However, across broad temperature gradients, where T_{crit} tends to increase with temperature (Feeley et al., 2020; O'Sullivan et al., 2017), spectral indications of photosynthetic stress may also increase (Seeley et al., 2025), potentially reversing the T_{crit} -spectral relationships observed here. Genotype by environment (GxE) interactions, such as those previously found in *Populus fremontii* (Corbin et al., 2024; Seeley et al., 2025), may further complicate predictions across growing conditions and genetic diversity. However, high-resolution airborne data (e.g., ≤1 m) collected in relatively similar environmental conditions—especially in extreme heat—may provide a viable path for capturing intraspecific variation in T_{crit} at canopy scales.

Leaf-level spectroscopy may also hold promise for high-throughput T_{crit} screening in common gardens or other controlled settings, where shared conditions minimize the impact of environmental noise. Although such approaches may capture only a subset of T_{crit} variability, they still may reliably distinguish relatively heat-tolerant plants from more sensitive ones, and do so at lower temperatures than is required by other phenotyping methods. For instance, in screening heat-tolerant wheat varieties, Sharma et al. (2015) found that the maximum quantum yield of PSII (F_v/F_m) required sustained extreme heat (40°C day/night for 72 hr) to differentiate tolerant and intolerant genotypes. In contrast, chlorophyll concentrations distinguished the same varieties under more realistic conditions (36/30°C day/night for 1 week). Leaf spectroscopy, by integrating signals from multiple chemical and physiological traits simultaneously (Doughty et al., 2011), might outperform approaches focusing on individual pigment concentrations, and therefore may offer a reliable means of detecting relative thermal tolerance at temperatures well below T_{crit}.

While leaf spectroscopy predicted T_{crit} with moderate accuracy in some contexts and spectral signatures were broadly consistent across data sets, we found that high-dimensional spectral models (e.g., PLSR) transferred poorly across species. This likely reflects context-specific relationships between reflectance and T_{crit}: complex models can capture subtle spectral features that correlate with thermal tolerance in a given taxon and environment, but those relationships may not hold elsewhere. In contrast, simpler, low-complexity spectral features sacrificed predictive power within individual data sets but generalized better to new contexts. For example, two-band indices (ChlNDI, PRI) achieved modestly high versus low T_{crit} classification across species and seasons (55%–63% accuracy). These results point to a likely tradeoff in using spectroscopy to inform leaf thermal tolerance. Complex spectral models trained within a given species and environment may be best suited for site- and species-specific phenotyping, whereas lower-dimensional features may be more useful in informing thermal tolerance in diverse species and contexts.

5. Conclusion

Our results show that leaf reflectance spectra can detect physiologically meaningful variation in PSII thermal tolerance (T_{crit}) within two contrasting foundation tree species. Spectral-T_{crit} relationships were strongest in visible and red-edge regions, suggesting a dominant role of photochemistry in linking leaf thermal tolerance and optical properties. Furthermore, while signatures were strongest under extreme heat, they were directionally similar across species and temperature conditions, suggesting a coherent signal that can either reflect variations in

heat stress mediated by variations in T_{crit}, or indicate mechanisms directly influencing tolerance. For example, lower chlorophyll concentrations likely indicate heat stress in less heat tolerant trees exposed to extreme heat, but may also reflect differences in pigment-protein complexes like LHCIIb, which can stabilize the thylakoid membrane and PSII under heat. The similarity of patterns across species from contrasting environments suggests shared biophysical constraints on photosynthesis and conserved pathways of thermal tolerance.

As these spectral signatures are consistent and interpretable across species and conditions, they may be broadly generalizable. This opens opportunities for scaling assessments of thermal tolerance using imaging spectroscopy or high-throughput spectral phenotyping. While spectral signals capture only part of the variation in T_{crit}, they may still provide reliable non-invasive indication of thermal tolerance variability, especially when collected in hot conditions.

Conflict of Interest

The authors declare no conflicts of interest relevant to this study.

Data Availability Statement

Data—Data and its descriptions to create all figures and tables in this paper are available in a Dryad data repository at the following URL: https://doi.org/10.5061/dryad.h9w0vt4w3. Software—All code and its descriptions to create all figures and tables in this paper are available in the same Dryad repository.

Acknowledgments
This research was supported by the National Science Foundation MacroSystems Biology program (DEB-2017877 and DEB-1340852). BCW acknowledges support from NASA's Future Investigators in NASA Earth and Space Science and Technology (FINESST) under award number 80NSSC24K1611. Special thanks to Susan Cordell, Don Drake, and Cliff Morden, as well as staff at the Volcano Research Station (University of Hawaii at Manoa) for helping to facilitate field measurements at the *M. polymorpha* common garden, and to our partners at the Bureau of Land Management at the *P. fremontii* common garden.

References

Asner, G. P., & Martin, R. E. (2008). Spectral and chemical analysis of tropical forests: Scaling from leaf to canopy levels. *Remote Sensing of Environment*, *112*(10), 3958–3970. Available at:. https://doi.org/10.1016/j.rse.2008.07.003

Asner, G. P., Martin, R. E., Anderson, C. B., & Knapp, D. E. (2015). Quantifying forest canopy traits: Imaging spectroscopy versus field survey. *Remote Sensing of Environment*, *158*, 15–27. https://doi.org/10.1016/j.rse.2014.11.011

Balzarolo, M., Peñuelas, J., Filella, I., Portillo-Estrada, M., & Ceulemans, R. (2018). Assessing ecosystem isoprene emissions by hyperspectral remote sensing. *Remote Sensing*, *10*(7), 1086. https://doi.org/10.3390/rs10071086

Behnke, K., Ehlting, B., Teuber, M., Bauerfeind, M., Louis, S., Hänsch, R., et al. (2007). Transgenic, non-isoprene emitting poplars don't like it hot. *The Plant Journal*, *51*(3), 485–499. https://doi.org/10.1111/j.1365-313X.2007.03157.x

Berry, J., & Bjorkman, O. (1980). Photosynthetic response and adaptation to temperature in higher plants. *Annual Review of Plant Physiology*, *31*(1), 491–543. https://doi.org/10.1146/annurev.pp.31.060180.002423

Bison, N. N., & Michaletz, S. T. (2024). Variation in leaf carbon economics, energy balance, and heat tolerance traits highlights differing timescales of adaptation and acclimation. *New Phytologist*, *242*(5), 1919–1931. https://doi.org/10.1111/nph.19702

Blasini, D. E., Koepke, D. F., Bush, S. E., Allan, G. J., Gehring, C. A., Whitham, T. G., et al. (2022). Tradeoffs between leaf cooling and hydraulic safety in a dominant arid land riparian tree species. *Plant, Cell and Environment*, *45*(6), 1664–1681. https://doi.org/10.1111/pce.14292

Bothwell, H. M., Keith, A. R., Cooper, H. F., Hull, J. B., Andrews, L. V., Wehenkel, C., et al. (2023). Microevolutionary processes in a foundation tree inform macrosystem patterns of community biodiversity and structure. *Forests*, *14*(5), 943. https://doi.org/10.3390/f14050943

Carter, G. A., & Knapp, A. K. (2001). Leaf optical properties in higher plants: Linking spectral characteristics to stress and chlorophyll concentration. *American Journal of Botany*, *88*(4), 677–684. https://doi.org/10.2307/2657068

Cawse-Nicholson, K., Townsend, P. A., Schimel, D., Assiri, A. M., Blake, P. L., Buongiorno, M. F., et al. (2021). NASA's surface biology and geology designated observable: A perspective on surface imaging algorithms. *Remote Sensing of Environment*, *257*, 112349. https://doi.org/10.1016/j.rse.2021.112349

Chavana-Bryant, C., et al. (2017). Leaf aging of Amazonian canopy trees as revealed by spectral and physiochemical measurements. *New Phytologist*, *214*(3), 1049–1063. https://doi.org/10.1111/nph.13853

Chen, S., Hong, X., Harris, C., & Sharkey, P. (2004). Sparse modeling using orthogonal forward regression with PRESS statistic and regularization. *IEEE Transactions on Systems, Man, and Cybernetics, Part B (Cybernetics)*, *34*(2), 898–911. https://doi.org/10.1109/TSMCB.2003.817107

Chicco, D., Warrens, M. J., & Jurman, G. (2021). The coefficient of determination R-squared is more informative than SMAPE, MAE, MAPE, MSE and RMSE in regression analysis evaluation. *PeerJ Computer Science*, *7*, e623. https://doi.org/10.7717/peerj-cs.623

Choi, J. Y., Dai, X., Alam, O., Peng, J. Z., Rughani, P., Hickey, S., et al. (2021). Ancestral polymorphisms shape the adaptive radiation of Metrosideros across the Hawaiian Islands. *Proceedings of the National Academy of Sciences*, *118*(37), e2023801118. https://doi.org/10.1073/pnas.2023801118

Chong, I.-G., & Jun, C.-H. (2005). Performance of some variable selection methods when multicollinearity is present. *Chemometrics and Intelligent Laboratory Systems*, *78*(1), 103–112. https://doi.org/10.1016/j.chemolab.2004.12.011

Coast, O., Posch, B. C., Rognoni, B. G., Bramley, H., Gaju, O., Mackenzie, J., et al. (2022). Wheat photosystem II heat tolerance: Evidence for genotype-by-environment interactions. *The Plant Journal*, *111*(5), 1368–1382. https://doi.org/10.1111/tpj.15894

Cook, A. M., Rezende, E. L., Petrou, K., & Leigh, A. (2024). Beyond a single temperature threshold: Applying a cumulative thermal stress framework to plant heat tolerance. *Ecology Letters*, *27*(3), e14416. https://doi.org/10.1111/ele.14416

Cooper, H. F., Grady, K. C., Cowan, J. A., Best, R. J., Allan, G. J., & Whitham, T. G. (2018). Genotypic variation in phenological plasticity: Reciprocal common gardens reveal adaptive responses to warmer springs but not to fall frost. *Global Change Biology*, *25*(1), 187–200. https://doi.org/10.1111/gcb.14494

Corbin, J. P. M., Best, R. J., Garthwaite, I. J., Cooper, H. F., Doughty, C. E., Gehring, C. A., et al. (2024). Hyperspectral leaf reflectance detects interactive genetic and environmental effects on tree phenotypes, enabling large-scale monitoring and restoration planning under climate change. *Plant, Cell and Environment*, *48*(n/a), n/a–1857. https://doi.org/10.1111/pce.15263

Cordell, S., Goldstein, G., Mueller-Dombois, D., Webb, D., & Vitousek, P. M. (1998). Physiological and morphological variation in Metrosideros Polymorpha, a dominant Hawaiian tree species, along an altitudinal gradient: The role of phenotypic plasticity. *Oecologia*, *113*(2), 188–196. https://doi.org/10.1007/s004420050367

Cushman, S. A., Max, T., Meneses, N., Evans, L. M., Ferrier, S., Honchak, B., et al. (2014). Landscape genetic connectivity in a riparian foundation tree is jointly driven by climatic gradients and river networks. *Ecological Applications*, *24*(5), 1000–1014. https://doi.org/10.1890/13-1612.1

Das, B., Sahoo, R. N., Pargal, S., Krishna, G., Verma, R., Chinnusamy, V., et al. (2018). Quantitative monitoring of sucrose, reducing sugar and total sugar dynamics for phenotyping of water-deficit stress tolerance in rice through spectroscopy and chemometrics. *Spectrochimica Acta Part A: Molecular and Biomolecular Spectroscopy*, *192*, 41–51. https://doi.org/10.1016/j.saa.2017.10.076

Demmig-Adams, B. (1990). Carotenoids and photoprotection in plants: A role for the xanthophyll zeaxanthin. *Biochimica et Biophysica Acta (BBA) - Bioenergetics*, *1020*(1), 1–24. https://doi.org/10.1016/0005-2728(90)90088-L

Demmig-Adams, B., Stewart, J. J., López-Pozo, M., Polutchko, S. K., & Adams III, W. W. (2020). Zeaxanthin, a molecule for photoprotection in many different environments. *Molecules*, *25*(24), 5825. https://doi.org/10.3390/molecules25245825

Dhami, N., & Cazzonelli, C. I. (2020). Environmental impacts on carotenoid metabolism in leaves. *Plant Growth Regulation*, *92*(3), 455–477. https://doi.org/10.1007/s10725-020-00661-w

Doughty, C. E., Asner, G. P., & Martin, R. E. (2011). Predicting tropical plant physiology from leaf and canopy spectroscopy. *Oecologia*, *165*(2), 289–299. https://doi.org/10.1007/s00442-010-1800-4

Doughty, C. E., & Goulden, M. L. (2009). Are tropical forests near a high temperature threshold? *Journal of Geophysical Research*, *114*(1). https://doi.org/10.1029/2007JG000632

Doughty, C. E., Keany, J. M., Wiebe, B. C., Rey-Sanchez, C., Carter, K. R., Middleby, K. B., et al. (2023). Tropical forests are approaching critical temperature thresholds. *Nature*, *621*(7977), 105–111. https://doi.org/10.1038/s41586-023-06391-z

Ellison, A. M., Bank, M. S., Clinton, B. D., Colburn, E. A., Elliott, K., Ford, C. R., et al. (2005). Loss of foundation species: Consequences for the structure and dynamics of forested ecosystems. *Frontiers in Ecology and the Environment*, *3*(9), 479–486. https://doi.org/10.1890/1540-9295(2005)003[0479:LOFSCF]2.0.CO;2

Feeley, K., Martinez-Villa, J., Perez, T., Silva Duque, A., Triviño Gonzalez, D., & Duque, A. (2020). The thermal tolerances, distributions, and performances of tropical montane tree species. *Frontiers in Forests and Global Change*, *3*, 25. https://doi.org/10.3389/ffgc.2020.00025

Feilhauer, H., Asner, G. P., Martin, R. E., & Schmidtlein, S. (2010). Brightness-normalized Partial Least Squares Regression for hyperspectral data. *Journal of Quantitative Spectroscopy and Radiative Transfer*, *111*(12), 1947–1957. https://doi.org/10.1016/j.jqsrt.2010.03.007

Fick, S. E., & Hijmans, R. J. (2017). WorldClim 2: New 1-km spatial resolution climate surfaces for global land areas. *International Journal of Climatology*, *37*(12), 4302–4315. https://doi.org/10.1002/joc.5086

Gamon, J. A., & Berry, J. A. (2012). Facultative and constitutive pigment effects on the Photochemical Reflectance Index (PRI) in sun and shade conifer needles. *Israel Journal of Plant Sciences*, *60*(1–2), 85–95. https://doi.org/10.1560/IJPS.60.1-2.85

Gamon, J. A., Peñuelas, J., & Field, C. B. (1992). A narrow-waveband spectral index that tracks diurnal changes in photosynthetic efficiency. *Remote Sensing of Environment*, *41*(1), 35–44. https://doi.org/10.1016/0034-4257(92)90059-S

Gamon, J. A., Serrano, L., & Surfus, J. S. (1997). The photochemical reflectance index: An optical indicator of photosynthetic radiation use efficiency across species, functional types, and nutrient levels. *Oecologia*, *112*(4), 492–501. https://doi.org/10.1007/s004420050337

Gamon, J. A., Somers, B., Malenovský, Z., Middleton, E. M., Rascher, U., & Schaepman, M. E. (2019). Assessing vegetation function with Imaging spectroscopy. *Surveys in Geophysics*, *40*(3), 489–513. https://doi.org/10.1007/s10712-019-09511-5

Gitelson, A. A., Zur, Y., Chivkunova, O. B., & Merzlyak, M. N. (2002). Assessing carotenoid content in plant leaves with reflectance spectroscopy. *Photochemistry and Photobiology*, *75*(3), 272–281. https://doi.org/10.1562/0031-8655(2002)0750272ACCIPL2.0.CO2

Green, R. O., et al. (2020). The Earth surface mineral dust source investigation: An Earth science imaging spectroscopy Mission. In *2020 IEEE aerospace conference. 2020* (pp. 1–15). IEEE Aerospace Conference. https://doi.org/10.1109/AERO47225.2020.9172731

Hartwell, S., Morino, K., Nagler, P. L., & Glenn, E. P. (2010). On the irrigation requirements of cottonwood (*Populus fremontii* and *Populus deltoides* var. *wislizenii*) and willow (*Salix gooddingii*) grown in a desert environment. *Journal of Arid Environments*, *74*(6), 667–674. https://doi.org/10.1016/j.jaridenv.2009.12.007

Havaux, M. (1998). Carotenoids as membrane stabilizers in chloroplasts. *Trends in Plant Science*, *3*(4), 147–151. https://doi.org/10.1016/S1360-1385(98)01200-X

Havaux, M., & Tardy, F. (1997). Thermostability and photostability of photosystem II in leaves of the Chlorina-f2 barley mutant deficient in light-harvesting chlorophyll a/b protein complexes. *Plant Physiology*, *113*(3), 913–923. https://doi.org/10.1104/pp.113.3.913

Heckathorn, S. A., Downs, C. A., Sharkey, T. D., & Coleman, J. S. (1998). The small, methionine-rich chloroplast heat-shock protein protects photosystem II electron transport during heat Stress1. *Plant Physiology*, *116*(1), 439–444. https://doi.org/10.1104/pp.116.1.439

Horler, D. N. H., Dockray, M., & Barber, J. (1983). The red edge of plant leaf reflectance. *International Journal of Remote Sensing*, *4*(2), 273–288. https://doi.org/10.1080/01431168308948546

Hueni, A., & Bialek, A. (2017). Cause, effect, and correction of field spectroradiometer interchannel radiometric steps. *IEEE Journal of Selected Topics in Applied Earth Observations and Remote Sensing*, *10*(4), 1542–1551. https://doi.org/10.1109/JSTARS.2016.2625043

Hultine, K. R., Allan, G. J., Blasini, D., Bothwell, H. M., Cadmus, A., Cooper, H. F., et al. (2020). Adaptive capacity in the foundation tree species *Populus fremontii*: Implications for resilience to climate change and non-native species invasion in the American Southwest. *Conservation Physiology*, *8*(1), coaa061. https://doi.org/10.1093/conphys/coaa061

Hüve, K., et al. (2006). Heat sensitivity of photosynthetic electron transport varies during the day due to changes in sugars and osmotic potential. *Plant, Cell and Environment*, *29*(2), 212–228. https://doi.org/10.1111/j.1365-3040.2005.01414.x

Ikeda, D. H., Max, T. L., Allan, G. J., Lau, M. K., Shuster, S. M., & Whitham, T. G. (2017). Genetically informed ecological niche models improve climate change predictions. *Global Change Biology*, *23*(1), 164–176. https://doi.org/10.1111/gcb.13470

IPCC. (2021). Climate change 2021: The physical science basis. *Contribution of working group I to the sixth assessment report of the intergovernmental panel on climate change*.

Jacquemoud, S., Verhoef, W., Baret, F., Bacour, C., Zarco-Tejada, P. J., Asner, G. P., et al. (2009). PROSPECT + SAIL models: A review of use for vegetation characterization. *Remote Sensing of Environment*, *113*, S56–S66. https://doi.org/10.1016/j.rse.2008.01.026

Jiang, J., Comar, A., Burger, P., Bancal, P., Weiss, M., & Baret, F. (2018). Estimation of leaf traits from reflectance measurements: Comparison between methods based on vegetation indices and several versions of the PROSPECT model. *Plant Methods*, *14*(1), 23. https://doi.org/10.1186/s13007-018-0291-x

Knight, C. A., & Ackerly, D. D. (2002). An ecological and evolutionary analysis of photosynthetic thermotolerance using the temperature-dependent increase in fluorescence. *Oecologia*, *130*(4), 505–514. https://doi.org/10.1007/s00442-001-0841-0

Koch, G. W., Amthor, J. S., & Goulden, M. L. (1994). Diurnal patterns of leaf photosynthesis, conductance and water potential at the top of a lowland rain forest canopy in Cameroon: Measurements from the Radeau des Cimes. *Tree Physiology*, *14*(4), 347–360. https://doi.org/10.1093/treephys/14.4.347

Kokaly, R. F. (2001). Investigating a physical basis for spectroscopic estimates of leaf nitrogen concentration. *Remote Sensing of Environment*, *75*(2), 153–161. https://doi.org/10.1016/S0034-4257(00)00163-2

Kress, E., & Jahns, P. (2017). The dynamics of energy dissipation and Xanthophyll conversion in arabidopsis indicate an indirect photoprotective role of zeaxanthin in slowly inducible and relaxing components of non-photochemical quenching of excitation energy. *Frontiers in Plant Science*, *8*, 2094. https://doi.org/10.3389/fpls.2017.02094

Liu, X., Wang, Z., Wang, W., Huang, Q., Zeng, Y., Jin, Y., et al. (2022). Origin and evolutionary history of populus (salicaceae): Further insights based on time divergence and biogeographic analysis. *Frontiers in Plant Science*, *13*, 1031087. https://doi.org/10.3389/fpls.2022.1031087

Martin, R. E., & Asner, G. P. (2009). Leaf chemical and optical properties of Metrosideros polymorpha across environmental gradients in Hawaii. *Biotropica*, *41*(3), 292–301. https://doi.org/10.1111/j.1744-7429.2009.00491.x

Martin, R. E., Asner, G. P., & Sack, L. (2007). Genetic variation in leaf pigment, optical and photosynthetic function among diverse phenotypes of Metrosideros polymorpha grown in a common garden. *Oecologia*, *151*(3), 387–400. https://doi.org/10.1007/s00442-006-0604-z

Mathur, S., Agrawal, D., & Jajoo, A. (2014). Photosynthesis: Response to high temperature stress. *Journal of Photochemistry and Photobiology B: Biology*, *137*, 116–126. https://doi.org/10.1016/j.jphotobiol.2014.01.010

Meireles, J. E., Cavender-Bares, J., Townsend, P. A., Ustin, S., Gamon, J. A., Schweiger, A. K., et al. (2020). Leaf reflectance spectra capture the evolutionary history of seed plants. *New Phytologist*, *228*(2), 485–493. https://doi.org/10.1111/nph.16771

Middleby, K. B., Cheesman, A. W., Hopkinson, R., Baker, L., Ramirez Garavito, S., Breed, M. F., & Cernusak, L. A. (2025). Ecotypic variation in leaf thermoregulation and heat tolerance but not thermal safety margins in tropical trees. *Plant, Cell and Environment*, *48*(1), 649–663. https://doi.org/10.1111/pce.15141

Moran, M. E., Aparecido, L. M. T., Koepke, D. F., Cooper, H. F., Doughty, C. E., Gehring, C. A., et al. (2023). Limits of thermal and hydrological tolerance in a foundation tree species (*Populus fremontii*) in the desert Southwestern United States. *New Phytologist*, *240*(6), 2298–2311. https://doi.org/10.1111/nph.19247

Nakagawa, S., Johnson, P. C. D., & Schielzeth, H. (2017). The coefficient of determination R2 and intra-class correlation coefficient from generalized linear mixed-effects models revisited and expanded. *Journal of the Royal Society Interface*, *14*(134), 20170213. https://doi.org/10.1098/rsif.2017.0213

Nie, Q., Dai, S., Feng, J., Kitudom, N., Fan, Z., Li, Z., & Lin, H. (2025). Light intensity alters thermal tolerance during heat and cold stress in canopy plant species. *Plant, Cell and Environment*, *48*(10), 7139–7149. https://doi.org/10.1111/pce.70002

Ollinger, S. V. (2011). Sources of variability in canopy reflectance and the convergent properties of plants. *New Phytologist*, *189*(2), 375–394. https://doi.org/10.1111/j.1469-8137.2010.03536.x

O'sullivan, O. S., Heskel, M. A., Reich, P. B., Tjoelker, M. G., Weerasinghe, L. K., Penillard, A., et al. (2017). Thermal limits of leaf metabolism across biomes. *Global Change Biology*, *23*(1), 209–223. https://doi.org/10.1111/gcb.13477

Penuelas, J. (1995). Semi-empirical indices to assess carotenoids/chlorophyll a ratio from leaf spectral reflectance. Retrieved from https://www.academia.edu/18561446/Semi_empirical_indices_to_assess_carotenoids_chlorophyll_a_ratio_from_leaf_spectral_reflectance

Peñuelas, J., Filella, I., & Gamon, J. A. (1995). Assessment of photosynthetic radiation-use efficiency with spectral reflectance. *New Phytologist*, *131*(3), 291–296. https://doi.org/10.1111/j.1469-8137.1995.tb03064.x

Posch, B. C., Bush, S. E., Koepke, D. F., Schuessler, A., Anderegg, L. L., Aparecido, L. M., et al. (2024). Intensive leaf cooling promotes tree survival during a record heatwave. *Proceedings of the National Academy of Sciences*, *121*(43), e2408583121. https://doi.org/10.1073/pnas.2408583121

Posch, B. C., Hammer, J., Atkin, O. K., Bramley, H., Ruan, Y. L., Trethowan, R., & Coast, O. (2022). Wheat photosystem II heat tolerance responds dynamically to short- and long-term warming. *Journal of Experimental Botany*, *73*(10), 3268–3282. https://doi.org/10.1093/jxb/erac039

Rajametov, S. N., Yang, E. Y., Cho, M. C., Chae, S. Y., Jeong, H. B., & Chae, W. B. (2021). Heat-tolerant hot pepper exhibits constant photosynthesis via increased transpiration rate, high Proline content and fast recovery in heat stress condition. *Scientific Reports*, *11*(1), 14328. https://doi.org/10.1038/s41598-021-93697-5

Rao, M. P., Davi, N. K., Magney, T. S., Andreu-Hayles, L., Nachin, B., Suran, B., et al. (2023). Approaching a thermal tipping point in the Eurasian boreal forest at its southern margin. *Communications Earth and Environment*, *4*(1), 1–10. https://doi.org/10.1038/s43247-023-00910-6

Richardson, A. D., Duigan, S. P., & Berlyn, G. P. (2002). An evaluation of noninvasive methods to estimate foliar chlorophyll content. *New Phytologist*, *153*(1), 185–194. https://doi.org/10.1046/j.0028-646X.2001.00289.x

Russo, S., Dosio, A., Graversen, R. G., Sillmann, J., Carrao, H., Dunbar, M. B., et al. (2014). Magnitude of extreme heat waves in present climate and their projection in a warming world. *Journal of Geophysical Research: Atmospheres*, *119*(22), 12500–12512. https://doi.org/10.1002/2014JD022098

Sastry, A., & Barua, D. (2017). Leaf thermotolerance in tropical trees from a seasonally dry climate varies along the slow-fast resource acquisition spectrum. *Scientific Reports*, *7*(1), 11246. https://doi.org/10.1038/s41598-017-11343-5

Schreiber, U., & Berry, J. A. (1977). Heat-induced changes of chlorophyll fluorescence in intact leaves correlated with damage of the photosynthetic apparatus. *Planta*, *136*(3), 233–238. https://doi.org/10.1007/BF00385990

Seeley, M. M., & Asner, G. P. (2023). Large-scale controls on the leaf economic spectrum of the overstory tree species Metrosideros polymorpha. *Remote Sensing*, *15*(19), 4707. https://doi.org/10.3390/rs15194707

Seeley, M. M., Thomson, E., Allan, G. J., Wiebe, B. C., Whitham, T. G., Hultine, K. R., et al. (2025). Disentangling heritability and plasticity effects on *Populus fremontii* leaf reflectance across a temperature gradient. *Oecologia*, *207*(11), 168. https://doi.org/10.1007/s00442-025-05806-0

Sharkey, T. D. (2005). Effects of moderate heat stress on photosynthesis: Importance of thylakoid reactions, rubisco deactivation, reactive oxygen species, and thermotolerance provided by isoprene. *Plant, Cell and Environment*, *28*(3), 269–277. https://doi.org/10.1111/j.1365-3040.2005.01324.x

Sharma, D. K., Andersen, S. B., Ottosen, C., & Rosenqvist, E. (2015). Wheat cultivars selected for high Fv/Fm under heat stress maintain high photosynthesis, total chlorophyll, stomatal conductance, transpiration and dry matter. *Physiologia Plantarum*, *153*(2), 284–298. https://doi.org/10.1111/ppl.12245

Shutilova, N., Semenova, G., Klimov, V., & Shnyrov, V. (1995). Temperature-induced functional and structural transformations of the photosystem II oxygen-evolving complex in spinach subchloroplast preparations. *Biochemistry & Molecular Biology International*, *35*(6), 1233–1243.

Slot, M., et al. (2020). Leaf heat tolerance of 147 tropical forest species varies with elevation and leaf functional traits, but not with phylogeny leaf heat tolerance of 147 tropical forest species varies with elevation and leaf functional traits, but not with phylogeny running head: Heat tolerance of tropical forest plants. https://doi.org/10.22541/au.160647491.19235940/v1

Stacy, E. A., Johansen, J. B., Sakishima, T., Price, D. K., & Pillon, Y. (2014). Incipient radiation within the dominant Hawaiian tree Metrosideros polymorpha. *Heredity*, *113*(4), 334–342. https://doi.org/10.1038/hdy.2014.47

Stacy, E. A., & Johnson, M. A. (2021). Floral variation across three varieties of the landscape-dominant tree Metrosideros polymorpha (Myrtaceae): Insights from a Hawaii Island common Garden. *International Journal of Plant Sciences*, *182*(1), 46–58. https://doi.org/10.1086/711848

Still, C. J., Page, G., Rastogi, B., Griffith, D. M., Aubrecht, D. M., Kim, Y., et al. (2022). No evidence of canopy-scale leaf thermoregulation to cool leaves below air temperature across a range of forest ecosystems. *Proceedings of the National Academy of Sciences*, *119*(38), e2205682119. https://doi.org/10.1073/pnas.2205682119

Still, C. J., Sibley, A., DePinte, D., Busby, P. E., Harrington, C. A., Schulze, M., et al. (2023). Causes of widespread foliar damage from the June 2021 Pacific Northwest Heat Dome: More heat than drought. *Tree Physiology*, *43*(2), 203–209. https://doi.org/10.1093/treephys/tpac143

Tafesse, E. G., Warkentin, T. D., Shirtliffe, S., Noble, S., & Bueckert, R. (2022). Leaf pigments, surface wax and spectral vegetation indices for heat stress resistance in pea. *Agronomy*, *12*(3), 739. https://doi.org/10.3390/agronomy12030739

Tiwari, R., Gloor, E., da Cruz, W. J. A., Schwantes Marimon, B., Marimon-Junior, B. H., Reis, S. M., et al. (2021). Photosynthetic quantum efficiency in south-eastern Amazonian trees may be already affected by climate change. *Plant, Cell and Environment*, *44*(7), 2428–2439. https://doi.org/10.1111/pce.13770

Tóth, S. Z., et al. (2011). The physiological role of ascorbate as Photosystem II electron donor: Protection against photoinactivation in heat-stressed leaves. *Plant Physiology*, *156*(1), 382–392. https://doi.org/10.1104/pp.110.171918

Valliere, J. M., Nelson, K. C., & Martinez, M. C. (2023). Functional traits and drought strategy predict leaf thermal tolerance. *Conservation Physiology*, *11*(1), coad085. https://doi.org/10.1093/conphys/coad085

Wang, K., Zhang, X., Goatley, M., & Ervin, E. (2014). Heat shock proteins in relation to heat stress tolerance of creeping bentgrass at different N levels. *PLoS One*, *9*(7), e102914. https://doi.org/10.1371/journal.pone.0102914

Wang, Q.-L., Chen, J. H., He, N. Y., & Guo, F. Q. (2018). Metabolic reprogramming in chloroplasts under heat stress in plants. *International Journal of Molecular Sciences*, *19*(3), 849. https://doi.org/10.3390/ijms19030849

Wang, Z., Chlus, A., Geygan, R., Ye, Z., Zheng, T., Singh, A., et al. (2020). Foliar functional traits from imaging spectroscopy across biomes in eastern North America. *New Phytologist*, *228*(2), 494–511. https://doi.org/10.1111/nph.16711

Winter, K., Garcia, M., & Virgo, A. (2025). Heat-induced F_0-fluorescence rise is not an indicator of severe tissue necrosis in thermotolerance assays of young and mature leaves of a tropical tree species, Calophyllum inophyllum. *Photosynthetica*, *63*(1), 46–50. https://doi.org/10.32615/ps.2025.004

Yamane, Y., Kashino, Y., Koike, H., & Satoh, K. (1997). Increases in the fluorescence Fo level and reversible inhibition of Photosystem II reaction center by high-temperature treatments in higher plants. *Photosynthesis Research*, *52*(1), 57–64. https://doi.org/10.1023/A:1005884717655

Zhou, R., Kjær, K. H., Rosenqvist, E., Yu, X., Wu, Z., & Ottosen, C. (2017). Physiological response to heat stress during seedling and Anthesis stage in Tomato genotypes differing in heat tolerance. *Journal of Agronomy and Crop Science*, *203*(1), 68–80. https://doi.org/10.1111/jac.12166

Zhu, L., Bloomfield, K. J., Hocart, C. H., Egerton, J. J., O'Sullivan, O. S., Penillard, A., et al. (2018). Plasticity of photosynthetic heat tolerance in plants adapted to thermally contrasting biomes. *Plant, Cell and Environment*, *41*(6), 1251–1262. https://doi.org/10.1111/pce.13133